

Superconductivity in infinite-layer nickelates

Yusuke Nomura¹, Ryotaro Arita^{1,2}

¹RIKEN Center for Emergent Matter Science, 2-1 Hirosawa, Wako, Saitama 351-0198, Japan

²Department of Applied Physics, University of Tokyo, 7-3-1 Hongo Bunkyo-ku, Tokyo 113-8656, Japan

E-mail: yusuke.nomura@riken.jp

June 2021

Abstract. The recent discovery of the superconductivity in the doped infinite layer nickelates $R\text{NiO}_2$ ($R=\text{La, Pr, Nd}$) is of great interest since the nickelates are isostructural to doped $(\text{Ca,Sr})\text{CuO}_2$ having superconducting transition temperature (T_c) of about 110 K. Verifying the commonalities and differences between these oxides will certainly give a new insight into the mechanism of high T_c superconductivity in correlated electron systems. In this paper, we review experimental and theoretical works on this new superconductor and discuss the future perspectives for the “nickel age” of superconductivity.

1. Introduction

Unconventional superconductivity in strongly correlated electron systems is one of the most central issues in condensed matter physics. In particular, the mechanism of high-temperature superconductivity in cuprates [1] has been the “holy grail” for more than 35 years, and many experimental and theoretical studies have been carried out. One promising strategy to unveil this long-standing puzzle is to compare cuprate superconductors with their variants and clarify which of the features of the cuprates plays a decisive role in superconductivity. However, the search for layered oxides with an electronic state similar to that of copper oxides is a highly non-trivial problem with a long history. In fact, a number of materials that are expected to be compatible with the keywords such as “two-dimensional,” “square lattice,” “single orbital,” and “near half-filling” have been investigated.

The cuprate parent compounds are a Mott insulator with d^9 filling in the copper $3d$ orbital (one hole per site in the hole picture). If there is particle-hole symmetry, a two-dimensional system with one d electron per site will be promising. Although titanium and vanadium oxides are candidates for a d^1 analog of cuprates, if we consider a similar crystal structure as cuprates, the electronic structure is not necessarily similar to that of cuprates: In the d^1 system in a typical octahedral crystal field, the electrons enter nearly degenerate t_{2g} orbitals, and the “single orbital” condition, one of the important keywords for cuprate superconductivity, is not easily satisfied [2–5]. Furthermore, the d_{xy} level needs to be lower than that of the d_{yz} and d_{zx} orbitals in contrast to the typical octahedral crystal field, and it requires extremely high pressure to realize such a situation [6]. It should also be noted that the t_{2g} orbitals do not point towards their ligands, so that the electronic structure associated with them, as well as their exchange interactions, is very different from those of the e_g orbitals.

In the cuprates, the onsite level of the $d_{x^2-y^2}$ orbital is higher than that of the $d_{3z^2-r^2}$ orbital. However, by lowering the position of the apical oxygen, the order can be reversed. Then a cuprate-like electronic state can be realized in the d^7 system with one electron in the e_g shell. Nickel oxides provide a playground for designing such d^7 analogs. However, the problem is how to control the position of the apical oxygen. Although such possibility has been explored considering artificial heterostructures, it seems difficult to achieve the ideal situation [7–9].

We can also consider a d^5 electron system where the orbital with the highest level in the t_{2g} shell becomes half-filling. Iridium oxides are such an example, and there are experimental reports suggesting the possibility of superconductivity [10, 11]. When

the spin-orbit coupling is strong as in the $5d$ electron systems, the t_{2g} bands split into $j_{\text{eff}} = 1/2$ and $j_{\text{eff}} = 3/2$ bands (j_{eff} : effective total angular momentum). The $j_{\text{eff}} = 1/2$ band becomes half-filling when the filling is d^5 , and an electronic structure similar to that of the cuprates may be realized. However, the energy splitting between the $j_{\text{eff}} = 1/2$ and $j_{\text{eff}} = 3/2$ bands is smaller than that between the $d_{x^2-y^2}$ and $d_{3z^2-r^2}$ orbitals in the cuprates, and it is not clear whether iridium oxides can be regarded as a $j_{\text{eff}} = 1/2$ single-orbital system [12–14].

In this way, the hunt for analogs of cuprate superconductors has not been very successful so far. However, recently, there has been significant progress from infinite-layer nickelates. The infinite-layer phase of the nickelates is realized by topotactic reduction, whose first experimental report by Crespin *et al.* [16, 17] (synthesis of LaNiO_2 powder) dates back to 1983, even before the discovery of the superconductivity in cuprates. Theoretically, in 1999, Anisimov *et al.* [18] argued that infinite-layer nickelates could be a direct d^9 analog of the cuprates (to be precise, the d -orbital filling deviates from d^9 , as described below), unlike the aforementioned attempts of d^{1-} , d^{7-} , and d^5 -analogs. Finally, in 2019, Li *et al.* reported superconductivity with a transition temperature of 9–15 K in thin-film samples of doped infinite-layer nickelate $\text{Nd}_{0.8}\text{Sr}_{0.2}\text{NiO}_2$ (Fig. 1) [15]. The infinite-layer nickelate superconducting family has now extended to doped PrNiO_2 [19, 20] and LaNiO_2 [21, 22]. It should be noted that, although Sr_2RuO_4 also exhibits unconventional superconductivity and is isostructural to La_2CuO_4 [23], its electronic structure is very different from that of cuprates in that all the three t_{2g} orbitals are involved with the formation of the Fermi surface. Thus, it is of great interest to consider how the electronic structure of the new superconductor resembles and differs from that of the cuprates and how the similarity with cuprates can be improved.

In this review, in Sec. 2, we first compare the crystal structure and local electronic configuration of the infinite-layer nickelates and the cuprates. Then, we move on to the current status of the experiments in Sec. 3. In Sec. 4, we discuss the electronic structure of the infinite-layer nickelates in more detail. Sec. 5 is devoted to the discussion on the essential degrees of freedom to describe the superconductivity. In Sec. 6, we show several candidates for expanding the nickelate superconducting family. Finally, we give a summary and outlook in Sec. 7. For other recent reviews, see Refs. [24–27].

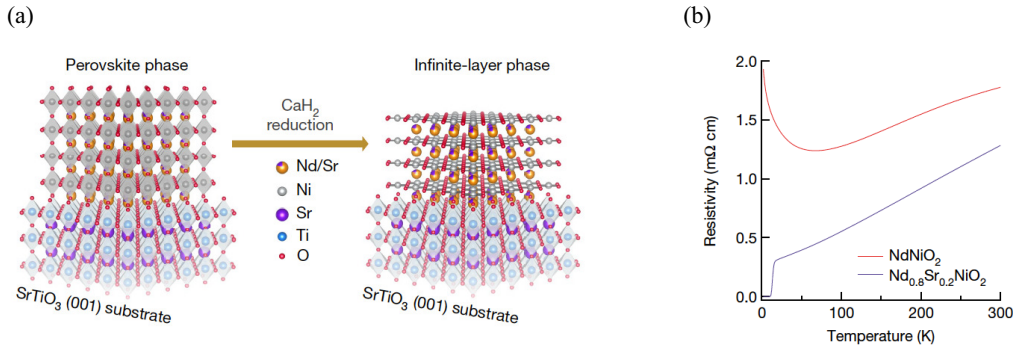


Figure 1. (a) Schematic figure for the crystal structures of $\text{Nd}_{0.8}\text{Sr}_{0.2}\text{NiO}_3$ (left) and $\text{Nd}_{0.8}\text{Sr}_{0.2}\text{NiO}_2$ (right) thin film samples on the SrTiO_3 substrate. The doped infinite-layer nickelates are prepared by topotactic reduction. (b) Resistivity as a function of temperature for NdNiO_2 and $\text{Nd}_{0.8}\text{Sr}_{0.2}\text{NiO}_2$ thin film samples. Reproduced from Ref. [15].

2. Crystal structure and crystalline electric field

In this section, let us first look into the crystal structure and local electronic configuration of the infinite-layer nickelate $R\text{NiO}_2$ ($R = \text{La}, \text{Pr}, \text{Nd}$) and compare with those of cuprates. The crystal structure of $R\text{NiO}_2$ is shown in Fig. 2(a). It has a layered structure, called an infinite-layer structure, with alternating NiO_2 and R layers. The structure is similar to that of the cuprates with a layered structure including CuO_2 planes. In fact, the corresponding infinite-layer cuprate $(\text{Sr}_{1-x}\text{Ca}_x)_{1-y}\text{CuO}_2$ also shows superconductivity with T_c of about 110 K [28].

In the infinite-layer structure, the apical oxygens are absent, and the composition changes from the well-known nickel oxide $R\text{NiO}_3$. A naive valence estimate shows that neodymium is a 3+ cation and oxygen is a 2- anion, giving nickel a 1+ valence. The corresponding occupation in the nickel 3d orbitals is d^9 , which is the same as that of the Cu^{2+} cations in the cuprate parent compounds. The square-planar crystal field [Fig. 2(b)] without the apical oxygens stabilizes the $d_{3z^2-r^2}$ orbital; its onsite level becomes comparable to those of the d_{xy} , d_{yz} , and d_{zx} orbitals (called t_{2g} orbitals in the octahedral environment). Therefore, the $d_{x^2-y^2}$ orbital is isolated from the other 3d orbitals in the energy diagram. Considering this crystal field together with the d^9 occupation, one expects that the half-filled $d_{x^2-y^2}$ -orbital system is realized in $R\text{NiO}_2$.

As mentioned in Sec. 1, “two-dimensional,” “square lattice,” “single orbital,” and “near half-filling” were the keywords to search for analogs of cuprates. The infinite-layer nickelate $R\text{NiO}_2$ is a candidate that satisfies all of these. The possible similarity between the nickelates and cuprates gives excitement in the field. The “nickel age” of superconductivity has thus started [24, 25].

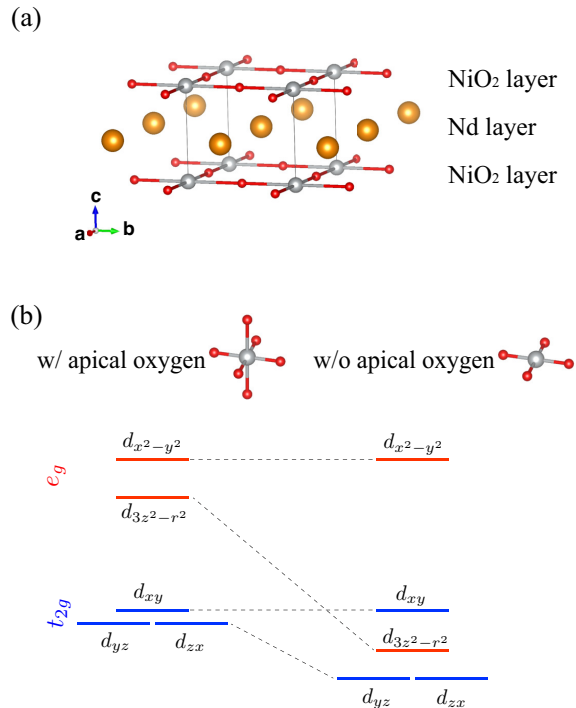


Figure 2. (a) The crystal structure of NdNiO_2 , and (b) the corresponding square-planar crystal field (right). In (b), for comparison, the crystal field with apical oxygen realized in, e.g., La_2CuO_4 is also shown (left). We use VESTA [29] to draw the crystal structure.

3. Experimental studies

3.1. Synthesis of superconducting materials

In the first report [15], D. Li *et al.* reported the superconductivity in the composition of $\text{Nd}_{0.8}\text{Sr}_{0.2}\text{NiO}_2$ ($T_c = 9\text{--}15$ K). The superconductivity has also been observed in doped PrNiO_2 thin film, $\text{Pr}_{1-x}\text{Sr}_x\text{NiO}_2$, with a maximum T_c of 14 K [19, 20]. All the superconducting samples are thin film samples on SrTiO_3

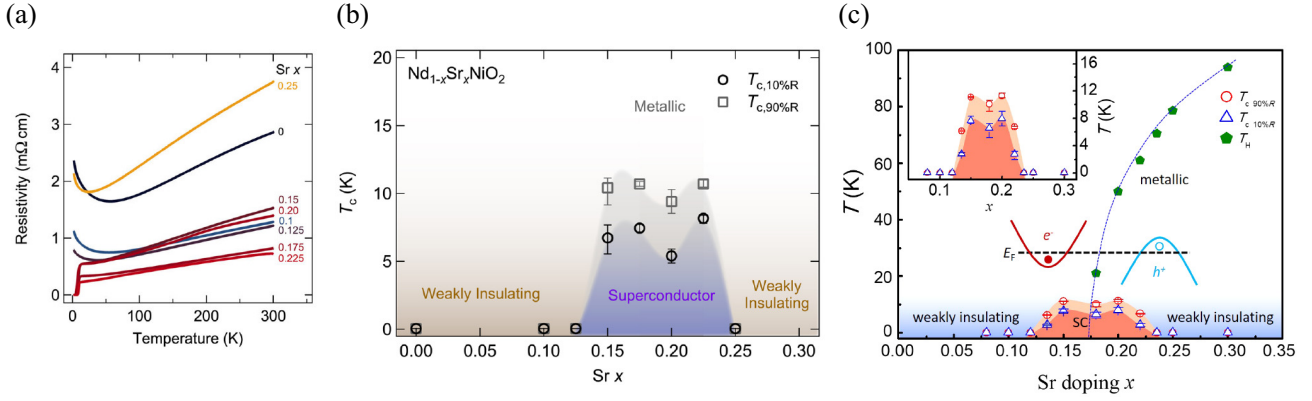


Figure 3. (a) Doping (x) dependence of the resistivity and (b,c) temperature-doping phase diagram of Nd_{1-x}Sr_xNiO₂ thin film samples on SrTiO₃ substrate. The panels (a,b) and (c) are reproduced from Refs. [30] and [31], respectively.

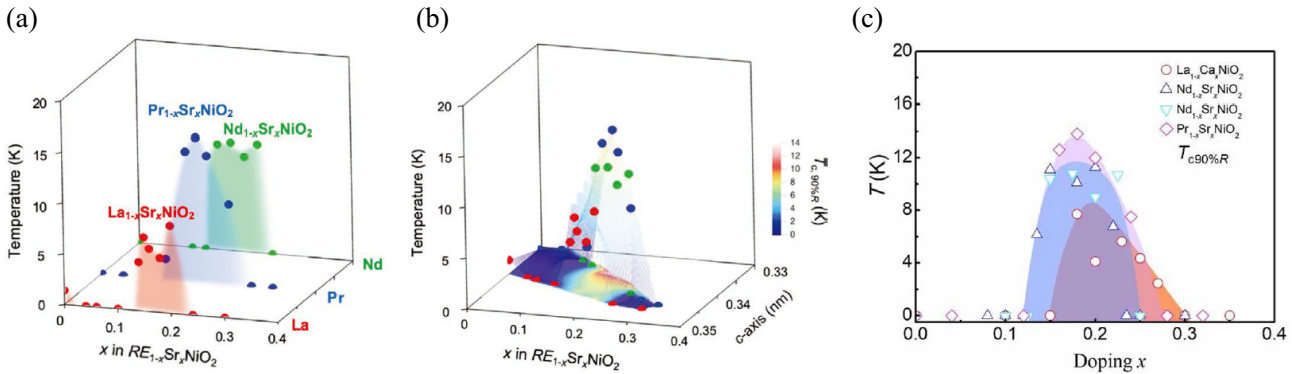


Figure 4. Comparison of the transition temperature among the superconducting infinite-layer nickelates [doped RNiO₂ ($R = \text{La, Pr, Nd}$) thin film samples]. The panels (a,b) and (c) are reproduced from Refs. [21] and [22], respectively.

substrates, and the details of the stable synthesis of film samples are discussed in Ref. [32].

It is worth noting that several other groups have now reproduced superconductivity in doped infinite-layer nickelate film samples [31, 33–36], although, in the early stage, there was a report of failure in reproducing the superconductivity in thin film samples [37]. The phase diagram of Nd_{1-x}Sr_xNiO₂ thin film with different strontium concentration x (Fig. 3) has been revealed independently by D. Li *et al.* [30] and S. W. Zeng *et al.* [31] (the groups of H. Y. Hwang and A. Ariando, respectively). As the latest news, the same two groups have independently observed the superconductivity in doped LaNiO₂ thin films [21, 22]. This is remarkable because the initial work had not succeeded in realizing superconductivity in doped LaNiO₂ [15] (see, e.g., Ref. [38] for the literature debating a possible reason for the absence of superconductivity). Furthermore, Ref. [21] also reported that there is a sign of superconductivity in undoped LaNiO₂ thin films [Fig. 4(a)]. This is interesting because NdNiO₂ and PrNiO₂ thin films do

not show superconductivity in their parent compounds. In contrast, undoped LaNiO₂ film samples in Ref. [22] are insulating from 300 K to 2K. It is desirable that the origin of the discrepancy between the two reports be clarified in the future.

As for bulk samples, to the best of our knowledge, there is no success in reproducing superconductivity. We refer to Refs. [39–42] for experimental effort on bulks (see also Ref. [43] for the discussion on the thermodynamical stability of the bulk infinite-layer nickelates).

3.2. Phase diagram

Figure 3 shows the phase diagram of Nd_{1-x}Sr_xNiO₂ thin films on the SrTiO₃ substrate. First, the resistivity of the parent material does not show a clear insulating behavior. The term “weakly insulating” refers to the slight upturn of the resistivity at low temperatures. Superconductivity is observed in the region where the strontium doping concentration is $0.125 \lesssim x \lesssim 0.25$, and a dome-shaped T_c is observed.

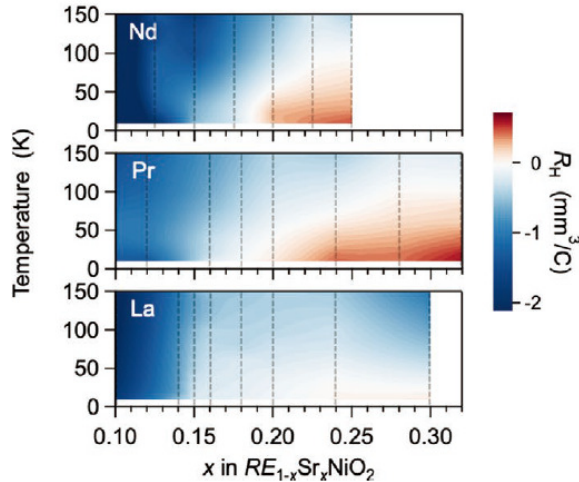


Figure 5. Contour maps of the Hall coefficients of doped NdNiO₂, PrNiO₂, and LaNiO₂ thin films. Reproduced from Ref. [21].

In the overdoped region, where the superconductivity disappears, the resistivity of Nd_{1-x}Sr_xNiO₂ increases at low temperatures, in contrast to the cuprates, which show metallic behavior. The increase of the resistivity may be due to, e.g., disorder, electron correlation, and secondary order parameters. The origin of this behavior is discussed in, e.g., Ref. [44] (see Sec. 3.3).

What is striking is the difference in the behavior of the parent materials between the nickelate and the cuprates. The cuprate parent compounds are an antiferromagnetic Mott insulator, whereas NdNiO₂ is not an insulator. Whereas the presence of the magnetic order in the thin film samples is not clear, the bulk powder NdNiO₂ samples show no long-range antiferromagnetic ordering down to low temperatures (1.7 K) [45]. We will discuss magnetism further in Sec. 4.2.2.

Figure 4 shows the comparison of T_c among the superconducting infinite-layer nickelates [21, 22]. One may be able to draw a unified phase diagram like in Fig. 4(b). It is an important future task to clarify the similarities and differences in more detail among superconducting family members.

3.3. Experiments to understand electronic structure, superconductivity, and magnetism

Other experimental facts are summarized as follows.

- Hall coefficient measurements of thin film samples suggest a coexistence of electron and hole carriers in Nd_{1-x}Sr_xNiO₂, and the sign of the Hall coefficient changes depending on the strontium concentration x and the temperature [30, 31]. A qualitatively similar sign change is also seen in

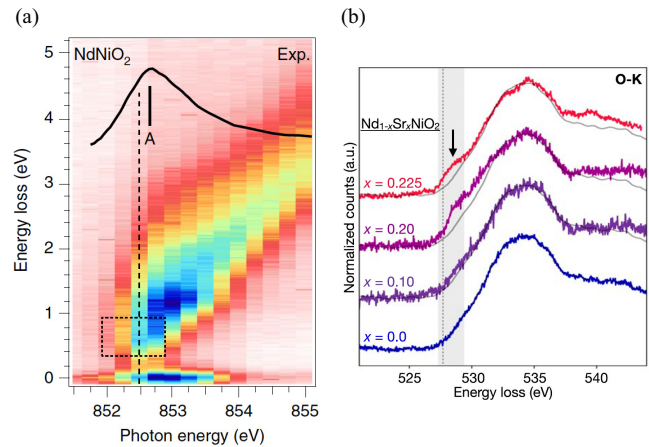


Figure 6. (a) Ni L₃-edge XAS (X-ray absorption spectroscopy) and RIXS (resonant inelastic X-ray scattering) of NdNiO₂ thin films. The XAS result is superimposed in the RIXS intensity map. The feature highlighted by the dashed box is interpreted as a signal for the Ni-Nd hybridization in Ref. [47]. (b) O K-edge EELS of Nd_{1-x}Sr_xNiO₂ thin films. A feature at around 528 eV in doped samples is attributed to $d^9\bar{L}$ states in Ref. [49]. Reproduced from (a) Ref. [47] and (b) Ref. [49].

doped PrNiO₂ and LaNiO₂ thin films [20–22] (Fig. 5).

- Experiments using the X-ray techniques and electron energy loss spectroscopy (EELS) reveal that the electronic states of the rare-earth layer show up around the Fermi level [Fig. 6(a)] and that NdNiO₂ is more close to the Mott-Hubbard regime in Zaanen-Sawatzky-Allen classification [46] compared to cuprates [47–50]. It suggests that the holes are mainly doped into nickel 3d orbitals (a signal for the doped holes in the oxygen 2p orbitals is also observed in the O K-edge EELS measurement, but the intensity is much smaller than that of the cuprates [49] [Fig. 6(b)]).
- Motivated by the discovery of the superconductivity, the magnetism of the bulk infinite-layer nickelates is reinvestigated using NdNiO₂ [48, 51], Nd_{0.85}Sr_{0.15}NiO₂ [52], LaNiO₂ [51, 53], and PrNiO₂ [51] samples. Recently, a RIXS measurement has been performed on NdNiO₂ thin film samples [54]. A quasi-two-dimensional magnetic excitation with a bandwidth of about 200 meV with large damping is observed (Fig. 7). It suggests a nonnegligible magnetic exchange interaction of about 64 meV on the NiO₂ layer [54], while a Raman experiment using bulk samples gave a smaller value of 25 meV [48]. The origin of the lack of a clear long-range magnetic order is also an open question. See Sec. 4.2.2 for more detailed discussion.
- Scanning tunneling microscope/spectroscopy (STM/STS)

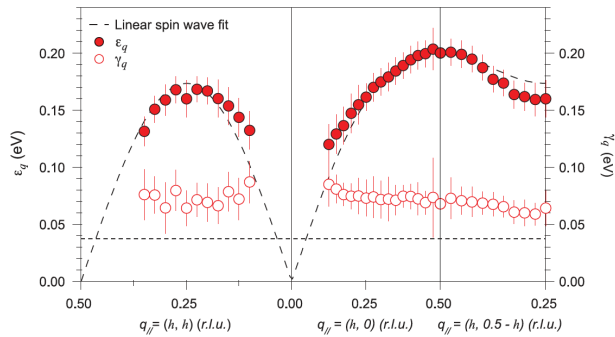


Figure 7. Dispersion of magnetic excitation in NdNiO₂ thin films inferred from the RIXS. The filled and open red circles indicate the energy of magnetic mode and damping factor, respectively. The dashed curve is the linear spin wave dispersion assuming the two-dimensional Heisenberg model with the nearest-neighbor coupling $J_1 = 63.6 \pm 3.3$ meV and the next-nearest-neighbor coupling $J_2 = -10.3 \pm 2.3$ meV. Reproduced from Ref. [54].

experiments on Nd_{1-x}Sr_xNiO₂ film samples observe, depending on the position of the inhomogeneous surface, *V*-shape or full-gap-type single-particle tunneling spectra (Fig. 8). In some cases, mixed spectra of the two components are observed [33]. The *V*-shape spectrum is compatible with the *d*-wave gap, whereas the full-gap-type spectrum suggests the *s*-wave symmetry. Ref. [33] interprets the coexistence of the different tunneling spectra by the different gap symmetries on different Fermi surfaces, while other explanations may also be plausible. The effects of the multi-orbital gap structure, the inhomogeneity, and surface reconstruction remain to be elucidated [55–58].

- The upper critical field of the doped NdNiO₂ thin film samples is investigated by two independent groups [59, 60]. Compared to the cuprates, the upper critical field shows a smaller spatial anisotropy. The analyses of the critical field suggest that the paramagnetic effect is dominant over the orbital effect (Pauli limit).
- When the system is in the Mott-Hubbard regime, the doped configuration becomes mainly *d*⁸, rather than *d*⁹ \underline{L} (\underline{L} denotes a hole in ligand oxygen) in the case of the charge-transfer regime. Ref. [61] has investigated the multiplet structure of the *d*⁸ configuration of doped NdNiO₂ film samples using the XAS and RIXS, and concluded that the orbital-polarized spin-singlet state, where the doped holes reside in the nickel $3d_{x^2-y^2}$ orbital, gives a dominant contribution. See Sec. 5.4 for the detailed discussion on the *d*⁸ multiplet structure.
- Ref. [62] has reported a diamagnetic response in superconducting Nd_{1-x}Sr_xNiO₂ film samples.

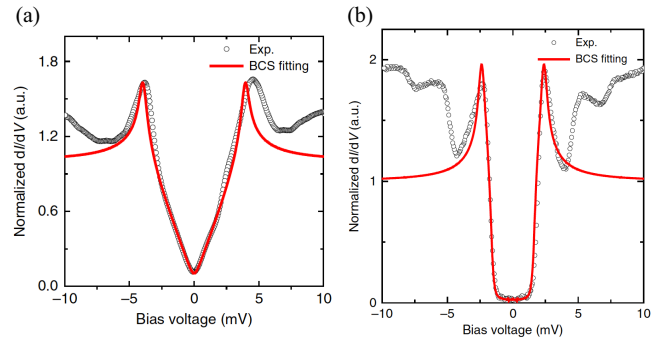


Figure 8. (a) A typical *V*-shape tunneling spectrum (black circles) and (b) a full-gap-type tunneling spectrum (black circles) measured at the surfaces of Nd_{1-x}Sr_xNiO₂ thin films. The spectrum depends on the position of the STM tip [33]. Reproduced from Ref. [33].

The film thickness dependence of the physical observables is also explored. The superconductivity is observed for different thickness (from 4.6 nm to 15.2 nm) samples, and thicker films tend to show a higher T_c . The change in the Hall coefficient and the XAS spectra depending on the thickness implies the modulation of the electronic structure due to the strain and interface effects.

- Normal state resistivity of Nd_{1-x}Sr_xNiO₂ film samples is studied in Ref. [44] by suppressing the superconductivity with out-of-plane magnetic fields. The upturn of the resistivity at low temperatures observed around $x = 0$ outside the superconducting dome persists in the field-induced normal state up to $x \approx 0.225$. At $x \approx 0.225$, a metallic transport is observed, but, above $x \approx 0.225$, the resistivity upturn shows up again. The systematic doping evolution of the transport property implies the intrinsic correlation effect and possible secondary order parameter, for which further investigations are required.

The consistency between these experimental facts and theory will be discussed in the following sections.

4. Electronic structure of infinite-layer nickelates

4.1. Insight from DFT calculations

In Sec. 2, we have discussed that the parent material, R NiO₂ (R =La, Pr, Nd), might be a single-orbital strongly-correlated system on a two-dimensional square lattice with half-filled $3d_{x^2-y^2}$ orbital, based on simple valence and crystal-field analyses. However, as we discuss in the following, this picture is not entirely true [63, 65–68]. Experimental facts reviewed in Sec. 3 also suggest that there should

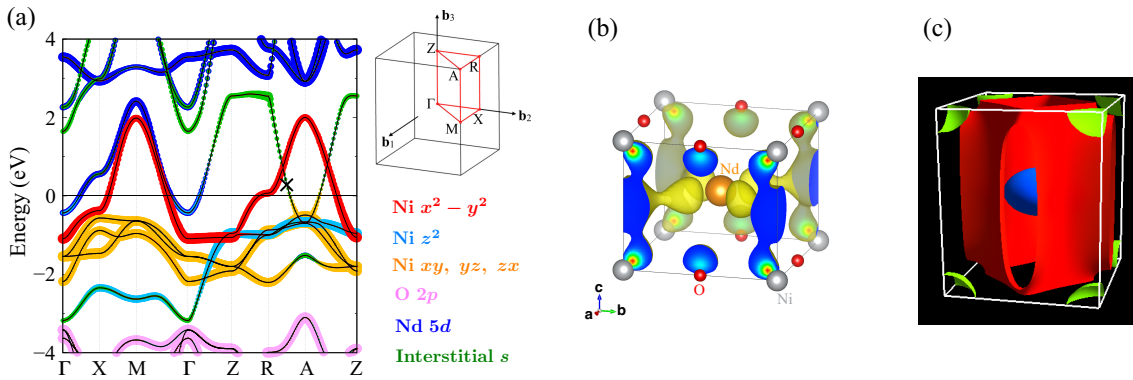


Figure 9. Electronic structure of bulk NdNiO_2 calculated using DFT with the GGA exchange-correlation functional. The lattice constants are taken from Ref. [45]. (a) Band structure of NdNiO_2 colored by the weight of each orbital (fat band). The neodymium $4f$ orbitals, which would form localized spins, are treated as “frozen core”. (b) Contour plot of the real-space electron density of the Bloch state marked with the \times symbol between the R and A points near the Fermi level in the panel (a). Orange, gray, and red spheres indicate the neodymium, nickel, and oxygen atoms, respectively. Yellow surfaces show an isosurface of the electron density. It has large weights around the missing apical oxygen site and neodymium site. Reproduced from Ref. [63]. (c) Fermi surface of NdNiO_2 . For the labels of high-symmetry k points in the Brillouin zone, see the panel (a). The nickel $3d_{x^2-y^2}$ orbital forms a large quasi-two-dimensional Fermi surface (red). The Fermi pocket around the Γ point (blue) has mainly neodymium $5d_{3z^2-r^2}$ character. The Fermi pocket near the A point (green) is derived from the bonding orbital between the interstitial s orbital and the neodymium $5d_{xy}$ orbital [see (b)]. The image was drawn using FermiSurfer [64].

be a deviation from the simple picture. In this section, we discuss the electronic structure of the infinite-layer nickelates through first-principles calculations.

Here, we restrict ourselves to bulk properties. The film thickness is on the order of 10 nm [32], so that there are several tens of NiO_2 layers in the sample. Furthermore, the superconductivity is robustly observed for samples with different thicknesses (from 4.6 nm to 15.2 nm) [62]. However, since the infinite-layer structure consists of charged layers, the reconstruction of the lattice and electronic structures is naturally expected at the interfaces and surfaces. Such effect is studied theoretically in Refs. [58, 69–73] (see also Ref. [27]). Experimental consideration has also started [62] (see Sec 3.3).

Figure 9(a) shows the band structure of the parent material NdNiO_2 (the first infinite-layer nickelate superconductor) calculated based on the density functional theory (DFT) with the generalized gradient approximation (GGA). In general, the band structure of strongly correlated materials deviates (at least quantitatively) from that of the DFT calculation due to electron correlation effects (mass renormalization, Mott-gap opening, and so on), especially near the Fermi level [75]. However, to see the global energy structure, the DFT-GGA calculations give a good starting point. See Sec. 4.2.1 for the discussion of correlation effects beyond the DFT.

The analysis of the band character near the Fermi level (Fig. 9) shows that the nickel $3d_{x^2-y^2}$ orbital creates a large Fermi surface. This is in agreement with the prediction of Sec. 2, and is a common feature

with the cuprates. Also, consistently with the crystal-field analysis in Sec. 2, the $3d_{x^2-y^2}$ orbital has the highest onsite level among the nickel $3d$ orbitals, and the $3d_{x^2-y^2}$ band is isolated from the other $3d$ bands in the energy space.

However, there is a discrepancy from the naïve expectation shown in Sec. 2. Besides the large Fermi surface of the nickel $3d_{x^2-y^2}$ orbital, additional Fermi pockets exist near the $\Gamma(0,0,0)$ and $A(\pi/a, \pi/a, \pi/c)$ points [Figs. 9(a) and 9(c)]. The Fermi pocket around the Γ point is formed by the rare-earth $5d_{3z^2-r^2}$ orbital with nickel $3d_{3z^2-r^2}$ orbital being hybridized [65, 66]. This fact may make nickel $3d_{3z^2-r^2}$ orbital active at the parent compound [65].

The origin of the Fermi pocket around the A point is referred to as the rare-earth $5d_{xy}$ orbital [67, 68] or the interstitial s orbital at the apical site [76]. In reality, the bonding orbital is formed between these two orbitals [63] [Fig. 9(b)]: At the A point, there is a large bonding-antibonding energy splitting of more than 10 eV [77], and the bonding part forms the additional Fermi pocket. This bonding orbital can be described either by $5d_{xy}$ -like Wannier orbital centered at the rare-earth site or the s -like orbital centered at the interstitial apical site; therefore, both pictures can be applied [63].

In most materials, interstitial-orbital bands appear far away from the Fermi level on the unoccupied side. However, in NdNiO_2 , the interstitial orbital at the apical site is stabilized because there is a space to gain the kinetic energy thanks to the absence of apical oxygen, and negatively-charged electrons feel an at-

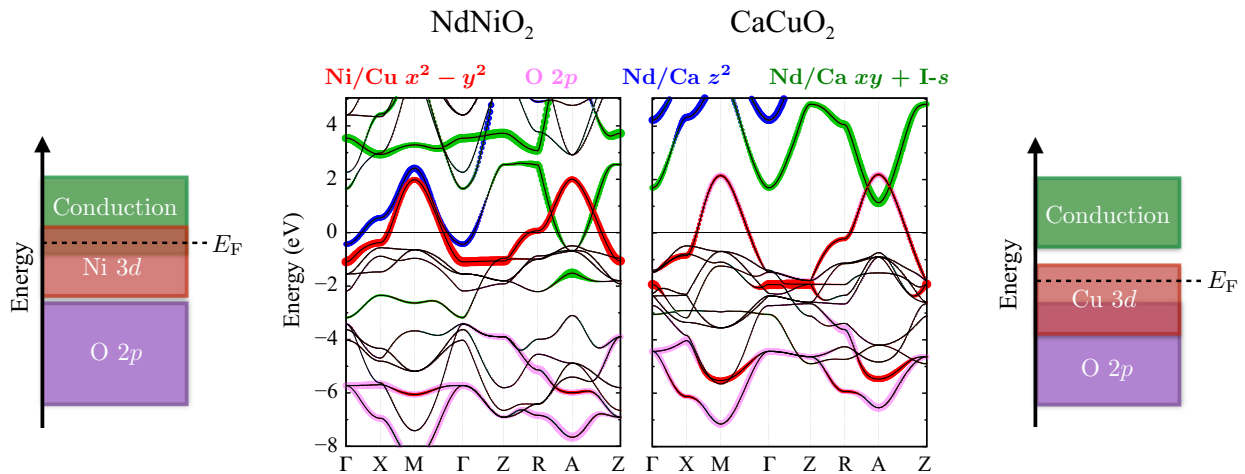


Figure 10. Comparison of the DFT-GGA band structures between NdNiO_2 and CaCuO_2 . Weights of nickel/copper $3d_{x^2-y^2}$ orbital, oxygen $2p$ orbitals hybridized with $3d_{x^2-y^2}$ orbitals in $\text{NiO}_2/\text{CuO}_2$ planes, neodymium/calcium $d_{3z^2-r^2}$ orbitals, and sum of neodymium/calcium d_{xy} and interstitial s (l - s orbital, l stands for interstitial) contributions are shown as fat bands. Note that the fat bands for the oxygen $2p$ orbitals here are limited to those hybridized with the $3d_{x^2-y^2}$ orbitals (p_x orbital of the oxygen in the x -direction and p_y orbital of oxygen in the y -direction), whereas, in Fig. 9, the fat bands were drawn for all the oxygen $2p$ orbitals. The lattice parameters of CaCuO_2 are taken from Ref. [74]. The figure is created inspired by the comparison between LaNiO_2 and CaCuO_2 shown in Refs. [65,66].

traction from the surrounding nickel and neodymium cations †. The neodymium $5d$ and interstitial- s orbitals are both located in the neodymium layer, and will henceforth be referred to collectively as Nd-layer orbitals (or more generally, rare-earth-layer orbitals).

Because the rare-earth-layer orbitals form the additional Fermi pockets, the nickel $3d_{x^2-y^2}$ orbital deviates from the half-filling even in the parent compound (occupation of the nickel $3d$ orbitals is not d^9) [65]. This “self-doping” effect is also seen in other infinite-layer compounds $R\text{NiO}_2$ (see, e.g., Refs. [78,79] for systematic investigation on the rare-earth element dependence). The self-doping marks one of the major differences from the cuprates, in which only the $3d_{x^2-y^2}$ band crosses the Fermi level (except for some materials) [65]. The DFT-level estimates suggest that the nickel $3d_{x^2-y^2}$ orbital is about 10% hole doped at the parent compound [63,66,67].

In order to further investigate the similarities and differences between the nickelates and cuprates, we show, in Fig. 10, the comparison of the band structures of NdNiO_2 and CaCuO_2 , a copper oxide with the same infinite-layer structure as NdNiO_2 (see Refs. [65,66] for detail). The weights of the nickel/copper $3d_{x^2-y^2}$ orbital, the oxygen $2p$ orbitals hybridized with the $3d_{x^2-y^2}$ orbital, and the neodymium/calcium-layer orbitals are also shown as “fat bands”.

In the case of CaCuO_2 , the copper $3d$ -orbital band is close to the oxygen $2p$ -orbital band, and the

† The band structure is similar to that of electrides, in which interstitial bands are occupied and the electrons themselves become negative ions.

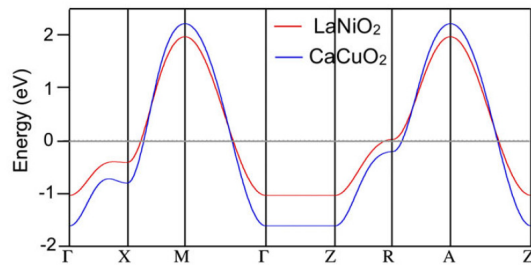


Figure 11. Tight-binding fit to the band with $3d_{x^2-y^2}$ character around the Fermi level for LaNiO_2 and CaCuO_2 . Reproduced from Ref. [66]. NdNiO_2 also has smaller bandwidth compared to CaCuO_2 (Fig. 10).

charge-transfer energy (the potential energy difference between the copper $3d$ orbital and the oxygen $2p$ orbital, which is the energy required for a hole to move from the copper site to the oxygen site) is small. On the other hand, in the case of NdNiO_2 , the valence of the nickel cation is about $1+$ and the attraction from the nucleus is small, which lifts the energy level of the $3d$ orbitals and makes the charge transfer energy larger than that of the cuprates. Due to the higher energy level of the $3d$ orbitals, the $3d_{x^2-y^2}$ band overlaps with the conduction band on the unoccupied side (originating from the Nd-layer orbitals). The self-doping has thus occurred. A larger charge transfer energy makes the hybridization between the nickel $3d_{x^2-y^2}$ and oxygen $2p$ orbitals smaller. As a result, the bandwidth of $3d_{x^2-y^2}$ band (more precisely, the

antibonding band between the nickel $3d_{x^2-y^2}$ and oxygen $2p$ orbitals) in NdNiO_2 is several tens percent smaller than that of CaCuO_2 (Fig. 11).

In Refs. [63, 67], the magnitude of the effective Coulomb interaction for the nickel $3d$ orbital has been estimated, indicating that NdNiO_2 is indeed strongly correlated. However, the presence of the self-doping naturally explains why the parent compound NdNiO_2 is not a Mott insulator despite the strong correlation. Also, the coexistence of the electron and hole carriers suggested by the Hall coefficient measurements is consistent with the multi-band nature around the Fermi level (hole carriers from the nickel $3d_{x^2-y^2}$ orbital and electron carriers from the Nd-layer orbitals).

In this section, we mainly discuss the electronic structure of NdNiO_2 . Importantly, a larger charge transfer energy compared to the cuprates and the existence of the self-doping are common features among LaNiO_2 , PrNiO_2 , and NdNiO_2 . Indeed, if we assume that the rare-earth $4f$ orbitals are localized and treat them as “frozen core”, the three compounds show qualitatively similar band structures [78, 79]. However, we note that the role of the rare-earth $4f$ orbitals has not been settled; A coupling between the rare-earth $4f$ orbitals and the orbitals around the Fermi level may affect the electronic structure around the Fermi level [80–83]. We will come back to this point in Sec. 5.2.

4.2. Correlation effect on the electronic structure

Here, we discuss the reconstruction of the electronic structure due to the correlation effects.

4.2.1. Calculations beyond DFT Many-body effects beyond the DFT level have been investigated using *GW*-type approach [77, 84, 85], DMFT(dynamical mean-field theory [86, 87])-type approach [38, 76, 88–103], and a combination of *GW*- and DMFT-type approaches [104, 105]. The main effects of the many-body correlations are the mass renormalization of the correlated orbitals as well as the relative shift of the orbital onsite levels. Frequency-dependent self-energy gives rise to incoherent parts in the spectral function (Fig. 12). Whereas the *GW*-type approach is good at describing spatially nonlocal correlations, the DMFT-type approach captures the spatially local correlations well. Within the DMFT, the Mott-Hubbard and charge-transfer physics, as well as the local multiplet structure arising from the crystal field and Hund’s coupling, can be studied.

It seems that most of the studies show a qualitative agreement in that the self-doping band robustly remains even with the many-body correlation effects. However, unfortunately, so far, there is no

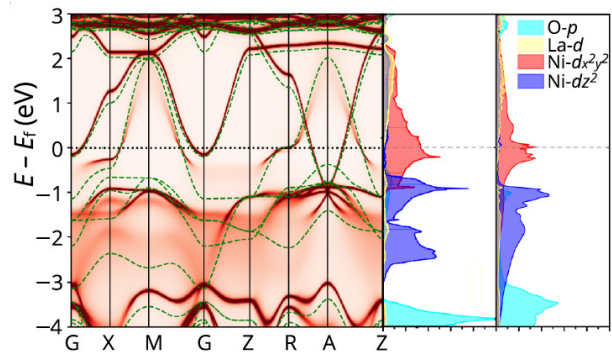


Figure 12. (Leftmost) The DFT+DMFT spectral function for LaNiO_2 . The green dashed curves show the DFT band dispersion. (Middle, Rightmost) Orbital-resolved spectral functions from DFT (middle) and DFT+DMFT (rightmost) calculations. Reproduced from Ref. [88].

consensus on the role of rare-earth-layer orbitals and the hole-doped electron configuration. Some works support the presence of Kondo physics arising from the coupling between the itinerant rare-earth-layer orbitals and correlated nickel $3d$ orbitals [76, 92]. Some papers propose the importance of Hund’s coupling and insist that the multi-orbital nature in the nickel $3d$ manifold is essential [89, 91–93, 100, 102, 104, 105]. On the other hand, Refs. [90, 95, 103] argue that the important correlation effect lies in the nickel $3d_{x^2-y^2}$ single band. The situation might be intermediate between these two [101]. Furthermore, Ref. [94] proposes that the charge-transfer physics is important as in the cuprates, while Refs. [90, 95, 103] are based on the Mott-Hubbard-type picture. These discrepancies may arise from different conditions (interaction strength, orbital basis, double-counting correction, and so on) employed in the DMFT calculations [96]. For the controversy on active degrees of freedom, we give an extended discussion in Sec. 5.

4.2.2. Magnetism Another effect of the electron correlation would be inducing some symmetry breaking: magnetism, stripe order, and so on (as for the superconductivity, we discuss in Sec. 5). Among them, magnetic instability is of great importance when we compare the infinite-layer nickelates with the cuprates.

So far, there exists no clear evidence for the magnetic long-range order in the parent compounds NdNiO_2 [45] and LaNiO_2 [106]. On the other hand, various theoretical studies have found magnetic solutions [65, 66, 76, 88, 93, 94, 97–100, 107–110] (Fig. 13). Although we do not go into detail further because of the lack of experimental evidence for the magnetic order in the parent compounds (for doped bulk $\text{Nd}_{0.85}\text{Sr}_{0.15}\text{NiO}_2$, an NMR study suggests the presence of short-range antiferromagnetic ordering below 40

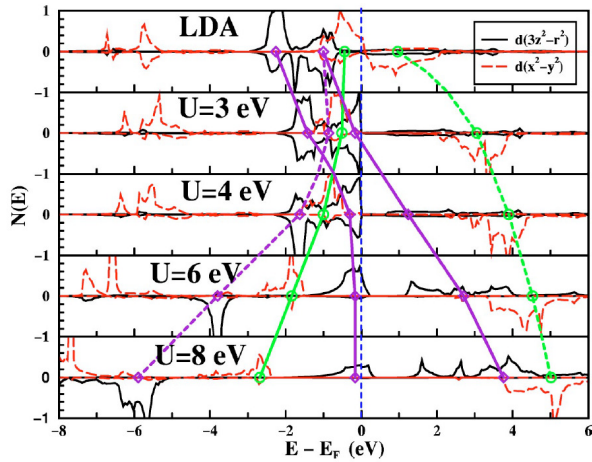


Figure 13. Density of states for nickel $3d_{x^2-y^2}$ and $3d_{3z^2-r^2}$ orbitals in the antiferromagnetic LDA+ U calculations for LaNiO_2 . The solid and dashed curves outline the path of the density of states of majority and minority spins, respectively, for $3d_{x^2-y^2}$ (green) and $3d_{3z^2-r^2}$ (purple) orbitals. Reproduced from Ref. [65].

K [52]), we emphasize that understanding the magnetism in the nickelates is one of the most urgent and important future tasks.

Another interesting related issue is the strength of the magnetic exchange coupling J , which may be one of the key factors for the high- T_c superconductivity [111]. The cuprates are a charge-transfer material, and J becomes large (~ 130 meV) due to the superexchange mechanism [111].

It is an interesting question whether the nickelates, which have larger charge-transfer energy and are more close to the Mott-Hubbard regime, exhibit large J or not. The J value for the infinite-layer nickelates is not settled: a Raman experiment using NdNiO_2 bulk samples estimated J to be much smaller (25 meV) than that of the cuprates [48]; on the other hand, a recent RIXS experiment on NdNiO_2 thin film samples gave a larger value of $J = 64(3)$ meV [54]. The J value is also scattered in theoretical estimates [78, 82, 88, 97–99, 107–109, 112–115]. One of the reasons for the discrepancy in theoretical estimates is ascribed to the ambiguity in calculating J : because the infinite-layer nickelate is not a Mott insulator due to the self-doping, there is ambiguity in mapping the system into the spin models. However, there seems to be an overall consensus that the J value is smaller than that of the cuprates. The problem is how small it is. This is an important question to be clarified in the future because it might be related to the difference in T_c between the nickelates and cuprates.

5. What are essential degrees of freedom for superconductivity?

In Sec. 4, we see that, although the self-doping and the large charge-transfer energy make a distinction between the nickelates and cuprates, they are similar in that the strongly correlated $3d_{x^2-y^2}$ orbitals have large Fermi surfaces at the DFT level. Then, the most interesting and fundamental question would be the pairing mechanism of superconductivity.

Ref. [63] calculated, from first principles, the electron-phonon coupling constant of NdNiO_2 and estimated the transition temperature T_c assuming the phonon Bardeen-Cooper-Schrieffer (BCS) [116] mechanism. The estimated T_c is less than 1 K. Thus, the phonon mechanism cannot explain the experimental T_c on the order of 10 K. This suggests that the superconductivity in doped NdNiO_2 originates from an unconventional mechanism (we note that the electron-phonon interactions may contribute to the superconductivity in cooperation with other mechanisms). Indeed, unconventional mechanisms have been proposed theoretically from the early stage [67, 68, 117]. Experimentally, the STM/STS experiment has observed a d -wave-like gap in some regions of the inhomogeneous surfaces of doped NdNiO_2 films [33] (see also Sec. 3.3).

When discussing unconventional mechanisms, it is helpful to construct an effective lattice Hamiltonian, such as the Hubbard model, t - J model, d - p model, or periodic Anderson model, for the electronic degrees of freedom near the Fermi level and analyze the superconductivity based on it. The effective Hamiltonian should reflect the crystal and electronic structures of the system. Then, what is the minimum model to describe the superconductivity in the infinite-layer nickelates (different models incorporate different physics such as Mott, Hund, and Kondo physics, as we discuss below)? In other words, what are the essential degrees of freedom for describing superconductivity? In this section, we will discuss this question.

So far, many different proposals have been made. However, there seems to be a consensus that the nickel $3d_{x^2-y^2}$ orbital is one of the essential degrees of freedom. Candidates for other key degrees of freedom include

- (i) the itinerant rare-earth-layer orbitals that form the additional Fermi pockets
 - (ii) the rare-earth $4f$ orbitals
 - (iii) the oxygen $2p$ orbitals that hybridize with $3d_{x^2-y^2}$ orbitals on the NiO_2 plane (p_x orbital of the oxygen in the x -direction and p_y orbital of oxygen in the y -direction)
 - (iv) nickel $3d$ orbitals other than the $3d_{x^2-y^2}$ orbital
- Each of these is discussed in the following.

5.1. Itinerant rare-earth-layer orbitals forming additional Fermi pockets

As we see in Sec. 4, the rare-earth-layer orbitals form Fermi pockets around the Γ and A points. The X-ray experiments on film samples consistently suggest that the rare-earth-layer orbitals are partially occupied [47]. Therefore, when discussing the symmetry of the superconductivity gap, we need to consider the gap functions on these Fermi surfaces. A key question, however, is whether the superconducting gaps on these bands are a byproduct of the superconductivity in the $3d_{x^2-y^2}$ band or whether they play an intrinsic role in the emergence of superconductivity. To put it a little differently, in discussing the properties such as superconductivity and magnetism, are the rare-earth-layer orbitals more than “charge reservoir” controlling the filling of the nickel $3d_{x^2-y^2}$ orbitals?

If the hybridization between the nickel $3d$ and rare-earth-layer orbitals is substantial, the rare-earth-layer orbitals are not only a charge reservoir, but they might give Kondo-like physics [113, 118]: The rare-earth-layer electrons have large bandwidth and couple to localized spins at nickel sites as itinerant conduction electrons. In this case, the increase in the electrical resistivity seen in NdNiO_2 from around 70 K [15] is interpreted as the Kondo effect [113, 118]. Following this picture, effective Hamiltonians that include both nickel $3d$ and rare-earth-layer orbitals have been proposed [47, 76, 113]. Ref. [56] has analyzed superconductivity based on the model proposed in Ref. [113] and shown pairing instabilities towards d , $d+is$, and s waves depending on the parameter region (Fig. 14).

The presence of Kondo physics is under debate: the recent experiments on the resistivity of magnetic-field-induced normal state using $\text{Nd}_{1-x}\text{Sr}_x\text{NiO}_2$ film samples have reported the resilience of the resistivity upturn against magnetic field and the positive magnetoresistance [44]. Ref. [44] poses a question on the Kondo scenario, whose effect is expected to be suppressed by the magnetic field. On the other hand, Ref. [119] observes negative magnetoresistance for LaNiO_2 film samples. The Kondo temperature is affected by the density of states and Fermi energy of the conduction bands and the strength of the Kondo coupling between the local spins and itinerant electrons [120]. The density of states of the rare-earth-layer orbital is not large [63]. As for the hybridization between the nickel $3d_{x^2-y^2}$ and rare-earth layer orbitals giving the Kondo coupling, some works argue that the hybridization is weak [90, 94], whereas others emphasize its importance [76, 92].

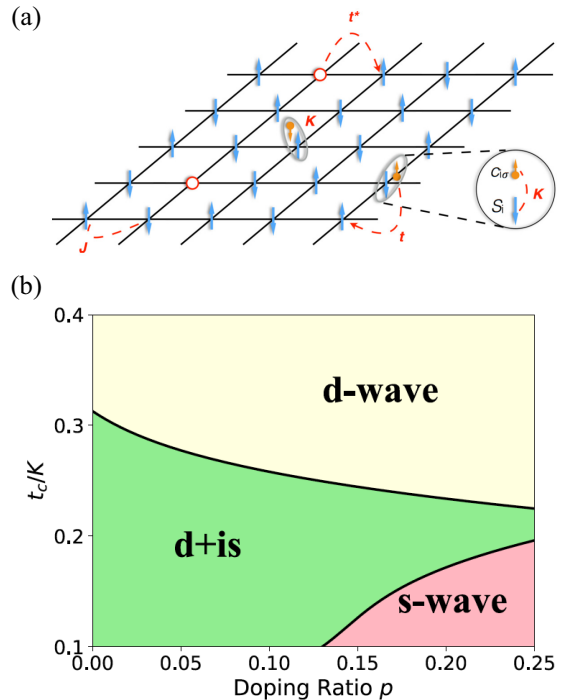


Figure 14. (a) Effective two-dimensional model on the square lattice proposed in Ref. [113]. Blue and orange arrows represent the nickel spins and rare-earth $5d$ electrons, respectively. J and K are the magnetic exchange coupling between the neighboring nickel spins and the Kondo coupling between the nickel spins and rare-earth $5d$ electrons, respectively. Red circles indicate nickel d^8 configuration (holon). t and t^* are the hopping integrals of doublons and holons, respectively. Reproduced from Ref. [113]. (b) Phase diagram of superconductivity obtained by generalized K - t - J model, where the Kondo coupling K to the itinerant electrons are added to the t - J model. t_c is the conduction electron hopping. The parameters in the t - J part is taken to be $t/K = 0.2$, $t^*/K = -0.05$, $J/K = 0.1$, where t , t^* , and J are nearest-neighbor hopping, next-nearest-neighbor hopping, and exchange coupling, respectively. Reproduced from Ref. [56].

5.2. Rare-earth $4f$ orbitals

At the moment, the role of the rare-earth $4f$ orbitals is an open question. Since the $4f$ orbitals are spatially localized, the bandwidth of $4f$ orbitals becomes small. Because of the correlation effect, the $4f$ electrons tend to be localized and form local magnetic moments. The disordered localized spins on the rare-earth layer may affect the transport property on the NiO_2 plane. Theoretically, the role of $4f$ orbitals has been investigated using the DFT-based calculations [80–83] and DFT+DMFT [102]. In particular, the DFT-based calculations suggest that an intraatomic interaction/hybridization between the rare-earth $4f$ and $5d$ orbitals may affect the energy level of the self-doping band [81, 83], thus changing the Fermi pocket size. A hybridization between the rare-earth $4f$ and nickel $3d$ orbitals is also discussed [80, 82]. On the other hand, the DFT+DMFT results show that

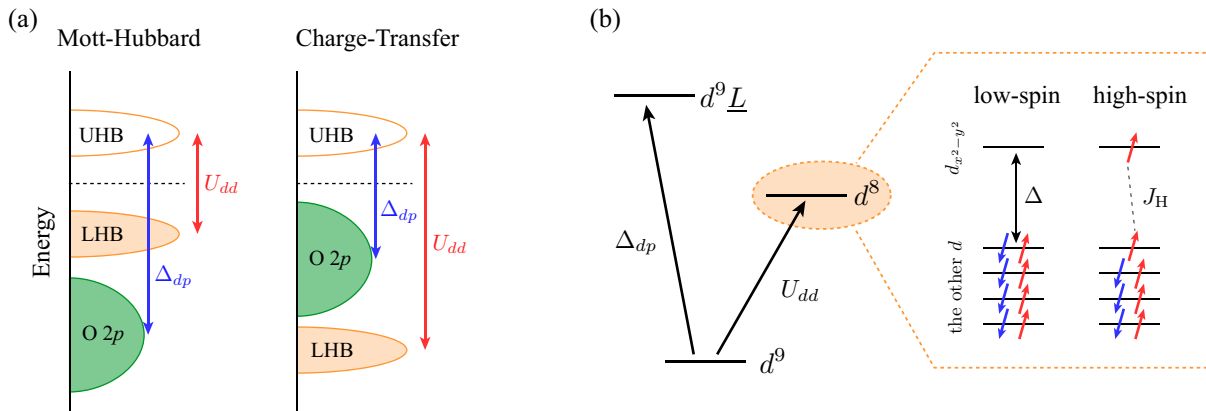


Figure 15. (a) Schematic figure showing the difference between a Mott-Hubbard insulator and a charge-transfer insulator. UHB and LHB are the upper Hubbard and lower Hubbard bands of the $3d$ orbitals, respectively. (b) Schematic energy diagram for the hole doping. There is a large energy scale competition between d^8 and $d^9 \underline{L}$ (U_{dd} vs Δ_{dp}). Within the d^8 configuration, a smaller energy scale competition exists between the low-spin ($S = 0$) and high-spin ($S = 1$) states (Δ vs J_H). Δ is the crystal-field splitting between the $3d_{x^2-y^2}$ orbital and the other $3d$ orbitals [see Fig. 2(b)]. J_H is Hund's coupling of the nickel $3d$ orbitals.

the bands around the Fermi level are almost unaffected by the rare-earth $4f$ orbitals [102]. Experimentally, on top of the superconductivity in doped NdNiO₂ and PrNiO₂ films with different $4f$ occupations, the superconductivity has been recently found in doped LaNiO₂ [21, 22] film samples, where the $4f$ orbitals are empty. The common observation of superconductivity irrespective of the filling of $4f$ orbitals would imply that the $4f$ degrees of freedom are not the main player in realizing superconductivity.

5.3. Oxygen $2p$ orbitals

It is of great importance to consider the role of oxygen $2p$ orbitals when comparing the cuprates and nickelates. A problem is to which orbitals the doped holes go (see Figs. 15 and 16). In the cuprates classified as a charge-transfer insulator in the Zaanen-Sawatzky-Allen phase diagram [46], the doped holes mainly enter the oxygen $2p$ orbitals because the charge-transfer energy Δ_{dp} is smaller than the $3d$ -orbital Hubbard interaction U_{dd} . Therefore, the electron configuration of the hole-doped cuprates is mainly $d^9 \underline{L}$, and the physics of Zhang-Rice singlet emerges [121].

On the other hand, in the case of the infinite-layer nickelates RNiO₂, Δ_{dp} is larger than that of the cuprates (see Sec. 4). This suggests that RNiO₂ is a Mott-Hubbard type material. The doped holes mainly go to the nickel $3d$ orbitals, and the doped electron configuration is mainly represented by d^8 (doping is expected to make the rare-earth-layer Fermi pockets smaller and weaken the self-doping effect). Note, however, that the hybridization between the nickel $3d_{x^2-y^2}$ orbital and the oxygen $2p$ orbitals is nonzero. Therefore, some holes should go to oxygen $2p$ orbitals [94, 109]. In fact, the O K-edge EELS

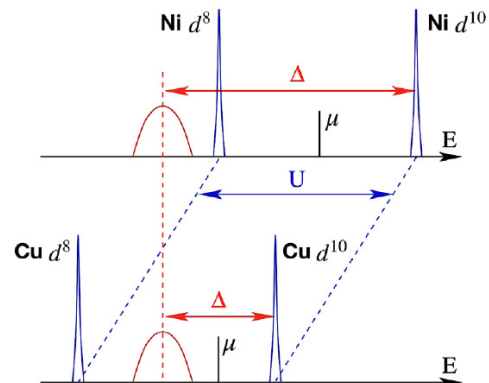


Figure 16. Schematic figure comparing the cuprates and nickelates assuming the charge-transfer energy Δ_{dp} (denoted as Δ in the figure) in the nickelates is much larger than that of the cuprates. The blue bands show Hubbard bands, while the red bands are oxygen $2p$ band with the pd hybridization being switched off. Reproduced from Ref. [112].

measurement has detected a signal of holes in the oxygen $2p$ orbitals, but the intensity is much smaller than that of the cuprates [49] (see also Sec. 3.3).

5.4. Other $3d$ orbitals

Based on the above discussion, the undoped d^9 configuration and the d^8 configuration with holes in the nickel $3d$ orbitals would be important in describing the superconductivity in the infinite-layer nickelates. When we follow this picture, an effective Hamiltonian would consist of nickel $3d$ orbitals (note that, in this case, the hybridization of the oxygen $2p$ orbitals with the nickel $3d_{x^2-y^2}$ orbital is taken into account by

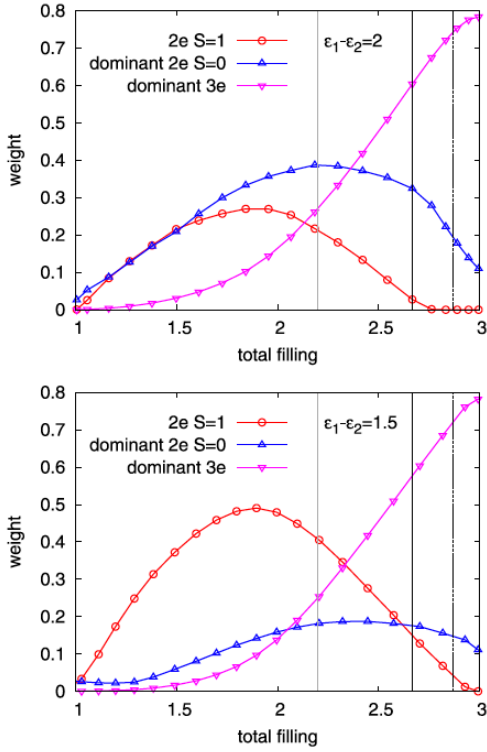


Figure 17. The DMFT results for the probability of local electron configurations for a two-orbital model mimicking nickel $3d_{x^2-y^2}$ and $3d_{3z^2-r^2}$ orbitals. The noninteracting density of states for these two orbitals is approximated by the semicircular density of states with the bandwidth of 3 ($3d_{x^2-y^2}$) and 2 ($3d_{3z^2-r^2}$). The Slater-Kanamori type interaction with $U = 2.6$, $U' = 1.3$, and $J = 0.5$ is employed with the Hubbard interaction U , the interorbital interaction U' , and the Hund's coupling J . ϵ_1 and ϵ_2 are the onsite level of $3d_{x^2-y^2}$ and $3d_{3z^2-r^2}$ orbitals, respectively. Reproduced from Ref. [89].

considering $3d_{x^2-y^2}$ -like Wannier orbitals centered at nickel sites with oxygen $2p$ tails). This raises a question: which model is more appropriate, the single-orbital or multi-orbital $3d$ model?

This can be understood as a competition between Hund's coupling and the crystal-field splitting, where the former (latter) favors the high-spin (low-spin) configuration [Fig. 15(b)]. If the crystal-field splitting between the $3d_{x^2-y^2}$ orbital and the other $3d$ orbitals is sufficiently large, the holes stay in the $3d_{x^2-y^2}$ orbitals. Then, the doped d^8 configuration takes the low-spin state ($S = 0$), and the single-orbital picture would be justified. If Hund's coupling induces the high-spin ($S = 1$) d^8 configuration, the multi-orbital model becomes indispensable. Several theoretical studies have argued that the multi-orbital nature cannot be ignored [89, 91–93, 100, 102, 104, 105, 110, 112, 122–124] (Fig. 17). On the other hand, Refs. [90, 95, 103] argue a single-orbital picture (for example, a recent DFT+DMFT study [103] has well reproduced the XAS, XPS, and

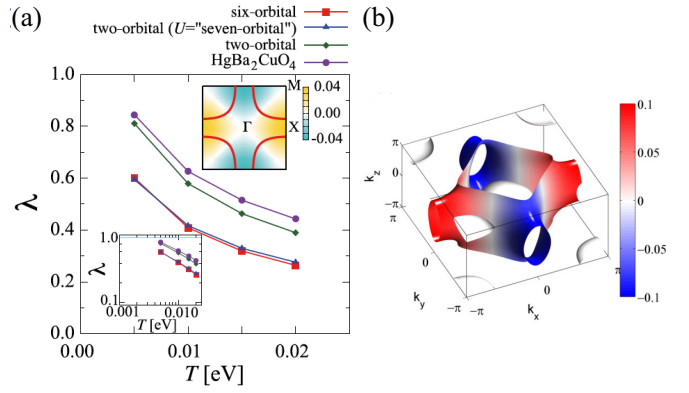


Figure 18. (a) Temperature evolution of the $d_{x^2-y^2}$ -wave pairing instability at 20 % hole doping for effective models of LaNiO_2 . λ is the eigenvalue of the Eliashberg equation. Three different models for LaNiO_2 are compared with the five orbital model of $\text{HgBa}_2\text{CuO}_4$ (see Ref. [67] for details). Ref. [67] argues that the superconducting instability in the nickelates is weaker than that of the cuprates because of a larger interaction and the resulting self-energy renormalization effect. The insets show λ - T log-log plot (bottom left) and the eigenfunction of the Eliashberg equation at $k_z = 0$ (top right). Reproduced from Ref. [67]. (b) The superconducting gap of $d_{x^2-y^2}$ -wave pairing at 20 % hole doping in the t - J model. Reproduced from Ref. [68].

RIXS spectra of NdNiO_2 in Refs. [47, 48, 61] with the low-spin ground state). An intermediate picture also exists: while the low-spin state is realized at low energy, the trace of Hund's coupling can be observed as dynamical orbital fluctuations at high frequencies [101]. Experimentally, Ref. [61] performed RIXS and XAS measurements using the doped NdNiO_2 film samples and suggested a low-spin character of the doped configuration (see also Ref. [125] and references therein for the situations for other d^8 nickelates with the square-planar environment).

5.5. Brief summary

To summarize the above discussion, most of the works view that the correlation effects in the nickel $3d_{x^2-y^2}$ orbital are important. Indeed, *ab initio* estimates of the effective Coulomb interactions within the nickel $3d$ manifold have suggested that the infinite-layer nickelates are strongly correlated systems [63, 67]. When one considers the nickel $3d_{x^2-y^2}$ orbital to be the most essential degrees of freedom, the d -wave pairing might be plausible: theoretically, spin-fluctuation-induced d -wave pairing for the nickel $3d_{x^2-y^2}$ orbital has been proposed [67, 68] (Fig. 18). From the standpoint of the single-orbital picture, the experimentally observed dome-like T_c [20–22, 30, 31] would be related to the change in superconducting instability as a function of the occupation of the nickel $3d_{x^2-y^2}$ orbital [90] (Fig. 19).

On the other hand, if we take a position that the

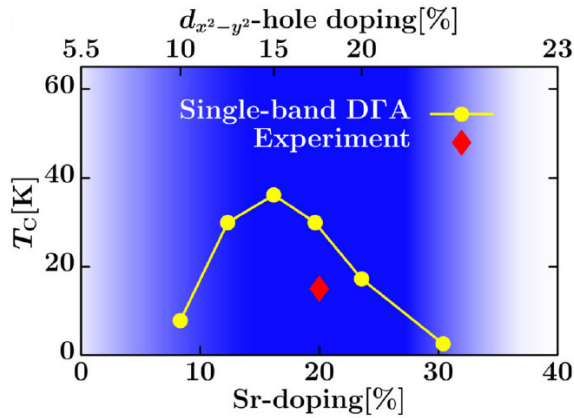


Figure 19. The superconducting transition temperature T_c of the d -wave pairing as a function of Sr-doping. The calculation is performed for a single-orbital Hubbard model using the dynamical vertex approximation (DGA). In the blue-shaded region, a single-orbital Hubbard model description is argued to be possible. Reproduced from Ref. [90].

multi-orbital nature is important, a comparison with iron-based superconductors may be interesting [100]. Enhanced dynamical spin fluctuations around spin-freezing (a phenomenon where the local moment is very slowly fluctuating, i.e., almost frozen) crossover induced by physical and effective Hund's coupling may be relevant to the superconductivity [89]. Strong-coupling-expansion type approach using the $3d$ multi-orbital model may help understanding the unconventional pairing [122–124]. Even when the Fermi surfaces of the other $3d$ orbitals do not exist, if other $3d$ bands exist just below the Fermi level (incipient band), such incipient bands can play a role in enhancing the superconductivity [57].

When the rare-earth-layer orbitals are active, they lead to another type of unconventional pairing through the Kondo coupling [56]. Even when they are not the main player in the development of superconductivity, they do form Fermi pockets. Thus, the superconducting gap should also be finite on these additional bands. The interactions between the nickel $3d$ orbitals and the rare-earth-layer orbitals would be an important factor in determining a gap structure for the additional Fermi pockets [55]. It is an important future task for experiments to reveal the gap structure on multiple Fermi pockets (a starting point is given by Ref. [33], see Sec. 3.3).

6. Searching for a new addition to the family

As we describe in Sec. 3, rare-earth infinite-layer nickelates show superconductivity for rare-earth elements of La, Pr, and Nd. Superconductivity may also appear for other rare-earth element cases, which

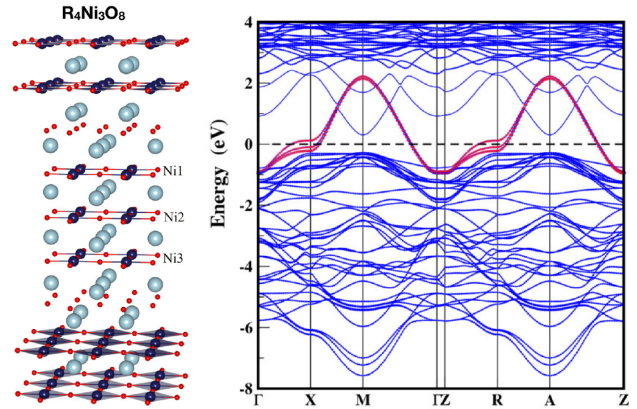


Figure 20. The crystal structure (left) and the DFT band dispersion (right) of a trilayer nickelate $R_4Ni_3O_8$. In the DFT calculation, $R=La$ is employed. The bands with dominant nickel $3d_{x^2-y^2}$ -orbital character are highlighted in red. Reproduced from Ref. [126].

is an interesting future task to be elucidated. Another intriguing issue is whether the superconductivity appears only in the infinite-layer structure or not. Here, we discuss several possible candidates for a new member of the family of nickel-based superconductors.

6.1. Multi-layer nickelates

The most natural extension of the infinite-layer nickelates would be the multi-layer square-planar nickelates [27, 126]. This is because the rare-earth infinite-layer nickelates are a special case ($n = \infty$) of the multi-layer square-planar nickelates $R_{n+1}Ni_nO_{2n+2}$. In the case of the cuprates, superconductivity appears both in infinite-layer and multi-layer structures [127].

Multi-layer square-planar nickelates with $n = 2$ and 3 had already been synthesized using the reduction process from the Ruddlesden-Popper parent compound $R_{n+1}Ni_nO_{3n+1}$ (see, e.g., Ref. [26] for a review). This situation is similar to the infinite-layer case, where $RNiO_2$ is obtained by the reduction from $RNiO_3$. An average nominal valence of the nickel ions in the $n = 3$ compound is $1.33+$ (i.e., $d^{8.67}$), which corresponds to the overdoped regime in the cuprates (see Fig. 20 for the crystal structure and the DFT band dispersion). Indeed, trilayer nickelates ($n = 3$) do not show superconductivity [128]. However, there is a signature for a large magnetic exchange coupling about 70 meV in the trilayer nickelate $La_4Ni_3O_8$, which makes multi-layer nickelates interesting reference systems between the cuprates and infinite-layer nickelates [129]. Increasing n would put the filling of nickel $3d$ orbital of multi-layer nickelates in the right place for possibly realizing superconductivity [24, 27]. In this respect, a notable experimental advance is a recent report of the

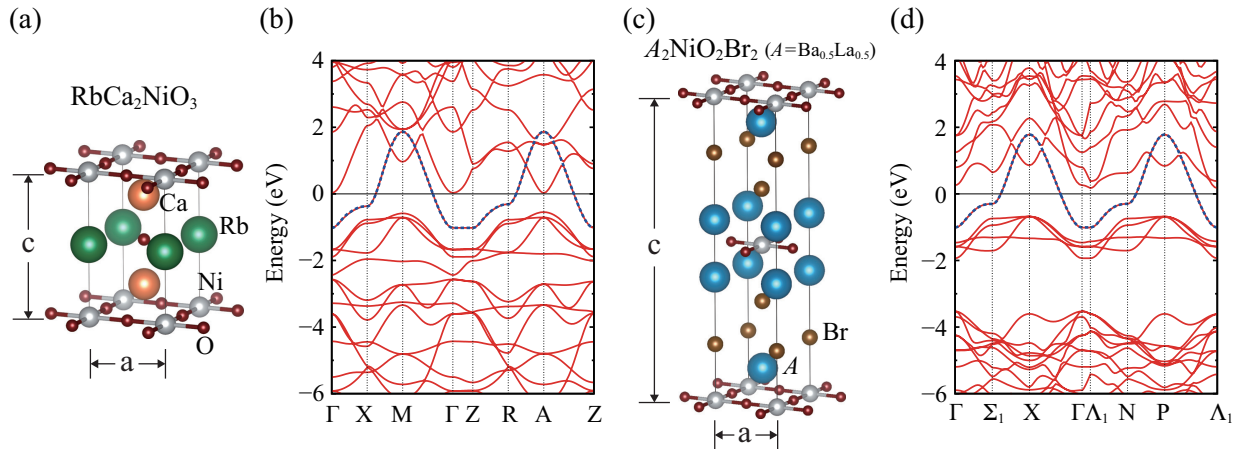


Figure 21. Two d^9 layered nickelates without self-doping proposed in Ref. [77]. Crystal structures of (a) $\text{RbCa}_2\text{NiO}_3$ and (c) $A_2\text{NiO}_2\text{Br}_2$ (A is a 2.5+-valent cation, here $\text{Ba}_{0.5}\text{La}_{0.5}$ is assumed), and (b,d) the corresponding DFT-GGA band structures. In (b) and (d), the \mathbf{k} path is consistent: $(0, 0, 0) \rightarrow (\pi/a, 0, 0) \rightarrow (\pi/a, \pi/a, 0) \rightarrow (0, 0, 0) \rightarrow (0, 0, \pi/c) \rightarrow (\pi/a, 0, \pi/c) \rightarrow (\pi/a, \pi/a, \pi/c) \rightarrow (0, 0, \pi/c)$ (The symbols are different because the primitive cells of $\text{RbCa}_2\text{NiO}_3$ and $A_2\text{NiO}_2\text{Br}_2$ are tetragonal and bace-centered tetragonal, respectively). The blue dotted curves are the Wannier band dispersion of an effective single-orbital model of the nickel $3d_{x^2-y^2}$ Wannier orbital with the oxygen- $2p$ tails. The band structure is metallic in the DFT-GGA calculation. However, they are expected to be Mott insulators if we properly take into account the correlation effects. Reproduced from Ref. [114].

epitaxial growth of the parent compound before the reduction, the Ruddlesden-Popper $R_{n+1}\text{Ni}_n\text{O}_{3n+1}$, up to $n = 5$ ($R = \text{La}$ [130] and $R = \text{Nd}$ [131]).

6.2. d^9 nickelates without self-doping

One of the major differences between the nickelates and cuprates is the presence of self-doping in the former. If the self-doping is eliminated, the Fermi surface topology of the nickelates will become more similar to the cuprates.

Ref. [77] systematically proposed layered nickelates by changing the composition of the layers between the NiO_2 layers (“block layer” [132], in the case of $R\text{NiO}_2$, the rare-earth layer corresponds to the block layer). Ref. [133] also introduced a similar idea: Indeed, one of the materials studied in Ref. [133] is also investigated in Ref. [77]. In order to avoid charge transfer between the block and NiO_2 layers, the material design was carried out using elements in the 1-3 groups that prefer closed shells. Furthermore, to keep a large crystal field splitting in the nickel $3d$ manifold, block layers without apical oxygens were considered. The structural stability of the designed nickelates was investigated from first-principles [77].

The designed nickelates tend to suppress the self-doping. Some of them are completely free from the self-doping, and only the nickel $3d_{x^2-y^2}$ band crosses the Fermi level in the DFT band structure [77]. The crystal and band structures of two such materials are shown in Fig. 21. In contrast with $R\text{NiO}_2$, these nickelates may satisfy all the keywords for cuprate analogs listed in Sec. 1, “two-dimensional,” “square lattice,” “single

orbital,” and “near half-filling”.

Since the strongly-correlated nickel $3d_{x^2-y^2}$ orbital becomes half-filling, the proposed self-doping-free d^9 nickelates are expected to become a Mott insulator, unlike the infinite-layer nickelates, which could not become a Mott insulator due to the self-doping [114]. The effective model for a Mott insulator is the spin-1/2 Heisenberg model with magnetic exchange interaction J . A first-principles estimate of the J value of the d^9 nickelates gives $J = 80\text{-}100$ meV [114], which is not far smaller than that of the cuprates (~ 130 meV [111]). The new nickelates showing a large magnetic exchange coupling J would provide an interesting playground to search for new superconductors close to the Mott-Hubbard regime in Zaanen-Sawatzky-Allen diagram [114].

In addition, the d^9 nickelates may provide a rare example of realizing a two-dimensional square-lattice Hubbard model, if the holes are doped into the $3d_{x^2-y^2}$ orbital [114]. Since the phase diagram of the doped Hubbard model on the square lattice is being reinvestigated thanks to a recent rapid advance in numerical techniques [134–136], the d^9 nickelates are of great interest as “testbed” materials [114].

We note a remarkable experimental advance also in synthesizing d^9 nickelates as well as multi-layer square-planar nickelates. Independently from the theoretical proposal [77], an experimental work [137] published around the same time has reported a successful synthesis of T'-type structure $\text{La}_2\text{NiO}_3\text{F}$. The same material has been investigated in Ref. [77] and is predicted to be dynamically stable; thus, the

experiment and theoretical prediction show a nice agreement. There is also an experimental report of the synthesis of a d^8 nickelate $\text{Sr}_2\text{NiO}_2\text{Cl}_2$ [138]. This is of great interest because $\text{Sr}_2\text{NiO}_2\text{Cl}_2$ has the same T-type structure as a theoretically proposed d^9 nickelate $A_2\text{NiO}_2\text{Br}_2$ (A is a 2.5+-valent cation) in Fig. 21(c), though the nickel valence is different (for the discussion of d^8 nickelates, see Sec. 6.3.1).

Another route for realizing d^9 nickelates would be nickel fluorides instead of nickel oxides [139]. Ref. [139] investigated infinite-layer fluoro-nickelates ANiF_2 with $A = \text{Li, Na, K, Rb, and Cs}$. Because fluorine is the most electronegative element, the energy difference between the nickel $3d$ and fluorine $2p$ orbitals becomes large. This places the fluoro-nickelates well inside the Mott-Hubbard regime and makes the nickel $3d_{x^2-y^2}$ bandwidth smaller (more strongly correlated).

There is also a proposal for nickel chalcogenides [140]. Ref. [140] argues that, compared to nickelates, nickel chalcogenides, such as NdNiS_2 , show more similar low-energy physics to cuprates and have stronger magnetic exchange coupling.

6.3. Other variants

6.3.1. d^8 nickelates The superconductivity in the infinite-layer nickelates emerges close to nickel d^9 filling, and thus the relation with the cuprates has been discussed intensively. Recently, there was a report on the superconductivity in nominally heavily-overdoped compound $\text{Ba}_2\text{CuO}_{3+\delta}$ [141]. Then, it would be interesting to expand the space for materials search. Refs. [57, 142] have investigated the layered nickelates around d^8 filling and discussed possible superconductivity.

6.3.2. Palladium and silver compounds As is discussed in Sec. 4, the bandwidth of nickel $3d_{x^2-y^2}$ orbital (or more precisely, anti-bonding orbital between nickel $3d_{x^2-y^2}$ orbital and oxygen $2p$ orbitals) is smaller compared to that of the cuprates. This makes the kinetic energy scale for the superconductivity smaller. To get a larger kinetic energy scale, palladium oxides (palladates), in which palladium $4d$ orbitals are more extended in space than nickel $3d$ orbitals, might be promising. Layered palladates around d^9 filling have been theoretically investigated in Refs. [143] and [77].

Silver-based compounds may also be interesting. A difficulty in using silver is that silver cation strongly favors 1+ valence. Using elements more electronegative than oxygen, Ag^{2+} can be realized. Ref. [144] studied the property of AgF_2 and shown that AgF_2 can be a cuprate-analog d^9 material with a large magnetic exchange coupling, reaching about 70 % of that of cuprates.

7. Summary and Outlook

The discovery of superconductivity in the doped infinite-layer nickelate $\text{Nd}_{0.8}\text{Sr}_{0.2}\text{NiO}_2$ was reported in August 2019. As a review at the initial stage of the research, we have reviewed the basics of the bulk electronic state.

In Sec. 4, we have discussed that the infinite-layer nickelate RNiO_2 is similar to the cuprates in that the nickel $3d_{x^2-y^2}$ orbital forms a strongly correlated system on the two-dimensional square lattice near the half-filling. However, a crucial difference from the cuprates is the presence of the self-doping: rare-earth-layer orbitals form additional Fermi pockets. In this sense, the parent compounds of the infinite-layer nickelates could be viewed as a material that fails to be a Mott insulator because of the self-doping. The superconductivity is most likely unconventional, and the correlation effect will play an important role.

Then, a question is what kind of correlation physics is essential (Sec. 5). If the itinerant rare-earth-layer orbitals are active, they would give rise to Kondo-like physics. If the holes are doped into oxygen $2p$ orbitals, the physics of Zhang-Rice singlet may emerge (Mott-Hubbard vs charge-transfer). When the holes reside within $3d$ manifold (Mott-Hubbard type), there should be a competition between the crystal-field splitting and Hund's coupling (low-spin vs high-spin). If the high-spin state is favored, Hund's physics comes into play. On the other hand, if the low-spin state is favored, Mott physics possibly masked by the self-doping would be important. We need more comprehensive experimental and theoretical investigations to clarify these points.

As for a future perspective, as one of the most important tasks, bulk superconducting samples are highly desired. If the superconductivity can only be realized in thin films, a difference between thin film and bulk samples needs to be discussed more seriously.

Another crucial question to be elucidated is the possibility of increasing T_c (currently, maximum T_c is about 15 K) in nickel-based superconductors. In this respect, the relation between superconductivity and other possible long-range-order instability needs to be clarified in the nickelates. In particular, the relation between superconductivity and magnetism would be one of the most urgent tasks to be investigated, considering the fact that the cuprates have an extraordinarily large magnetic exchange coupling of more than 100 meV. Although experiments detect a signature of magnetic fluctuations, so far, there is no clear evidence for long-range magnetic order in the infinite-layer parent compound RNiO_2 (see Sec. 3). The presence of the self-doping might be the origin of the absence of long-range order (note that the long-range order is quickly suppressed in the hole-doping

side of the cuprate phase diagram [145]). In this respect, d^9 nickelates without self-doping (see Sec. 6), if realized, would be an ideal material to investigate magnetism in the nickelates and compare it with that of the cuprates. An expected Mott insulating behavior eliminates the ambiguity in the mapping to spin model, and the magnetic exchange coupling is well defined.

To conclude, for sure, one needs more comprehensive experimental and theoretical efforts to get a complete picture of nickelate superconductivity. The nickelates nicely expand the playground for exploring unconventional superconductivity around the cuprate high- T_c superconductivity and provide excellent references to be compared with other unconventional superconductors. The establishment and understanding of superconductivity in nickelates will shed new light on the unresolved challenge of elucidating the superconducting mechanism in the correlated materials.

Note added. After submitting the manuscript, we became aware of intriguing experimental progress. Recently, superconductivity has been discovered in film samples of a quintuple-layer nickelate $\text{Nd}_6\text{Ni}_5\text{O}_{12}$ [146]. This is the first report of nickelate superconductivity other than in infinite-layer compounds (see Sec. 6.1). Also, charge-order and charge-density-wave instabilities in infinite-layer nickelates are discussed in recent works [147–149]. Interestingly, charge stripes, which couple to the spin degrees of freedom, had been found in a trilayer nickelate $\text{La}_4\text{Ni}_3\text{O}_8$ [150, 151]. Elucidating the systematic phase diagram of multi-layer and infinite-layer nickelates is a major challenge for the future.

Acknowledgements

We are grateful for fruitful discussions with Motoaki Hirayama, Terumasa Tadano, Takuya Nomoto, Motoharu Kitatani, Yoshihide Yoshimoto, and Kazuma Nakamura. We acknowledge the financial support by Grant-in-Aids for Scientific Research (JSPS KAKENHI) [Grant No. 20K14423 (YN), 21H01041 (YN), and 19H05825 (RA)] and MEXT as “Program for Promoting Researches on the Supercomputer Fugaku” (Basic Science for Emergence and Functionality in Quantum Matter —Innovative Strongly-Correlated Electron Science by Integration of “Fugaku” and Frontier Experiments—) (JPMXP1020200104).

- [1] J. G. Bednorz and K. A. Müller. Possible high T_c superconductivity in the Ba-La-Cu-O system. *Zeitschrift für Physik B Condensed Matter*, 64(2):189–193, 1986.
- [2] W.E. Pickett, D. Singh, D.A. Papaconstantopoulos, H. Krakauer, M. Cyrot, and F. Cyrot-Lackmann.

- Theoretical studies of Sr_2VO_4 , a charge conjugate analog of La_2CuO_4 . *Physica C: Superconductivity and its Applications*, 162-164:1433–1434, 1989.
- [3] Yoshiki Imai, Igor Solovyev, and Masatoshi Imada. Electronic Structure of Strongly Correlated Systems Emerging from Combining Path-Integral Renormalization Group with the Density-Functional Approach. *Phys. Rev. Lett.*, 95:176405, Oct 2005.
- [4] J. Matsuno, Y. Okimoto, M. Kawasaki, and Y. Tokura. Variation of the Electronic Structure in Systematically Synthesized Sr_2MO_4 ($M = \text{Ti}, \text{V}, \text{Cr}, \text{Mn}, \text{and Co}$). *Phys. Rev. Lett.*, 95:176404, Oct 2005.
- [5] Hongming Weng, Y. Kawazoe, Xiangang Wan, and Jinming Dong. Electronic structure and optical properties of layered perovskites Sr_2MO_4 ($M = \text{Ti}, \text{V}, \text{Cr}, \text{and Mn}$): An ab initio study. *Phys. Rev. B*, 74:205112, Nov 2006.
- [6] R. Arita, A. Yamasaki, K. Held, J. Matsuno, and K. Kuroki. Sr_2VO_4 and Ba_2VO_4 under pressure: An orbital switch and potential d^1 superconductor. *Phys. Rev. B*, 75:174521, May 2007.
- [7] J. Chaloupka and Giniyat Khaliullin. Orbital Order and Possible Superconductivity in $\text{LaNiO}_3/\text{LaMO}_3$ Superlattices. *Phys. Rev. Lett.*, 100:016404, Jan 2008.
- [8] P. Hansmann, Xiaoping Yang, A. Toschi, G. Khaliullin, O. K. Andersen, and K. Held. Turning a Nickelate Fermi Surface into a Cupratelike One through Heterostructuring. *Phys. Rev. Lett.*, 103:016401, Jun 2009.
- [9] M. J. Han, Xin Wang, C. A. Marianetti, and A. J. Millis. Dynamical Mean-Field Theory of Nickelate Superlattices. *Phys. Rev. Lett.*, 107:206804, Nov 2011.
- [10] Y. K. Kim, N. H. Sung, J. D. Denlinger, and B. J. Kim. Observation of a d -wave gap in electron-doped Sr_2IrO_4 . *Nature Physics*, 12(1):37–41, 2016.
- [11] Y. J. Yan, M. Q. Ren, H. C. Xu, B. P. Xie, R. Tao, H. Y. Choi, N. Lee, Y. J. Choi, T. Zhang, and D. L. Feng. Electron-Doped Sr_2IrO_4 : An Analogue of Hole-Doped Cuprate Superconductors Demonstrated by Scanning Tunneling Microscopy. *Phys. Rev. X*, 5:041018, Nov 2015.
- [12] Cyril Martins, Markus Aichhorn, Loïc Vaugier, and Silke Biermann. Reduced Effective Spin-Orbital Degeneracy and Spin-Orbital Ordering in Paramagnetic Transition-Metal Oxides: Sr_2IrO_4 versus Sr_2RhO_4 . *Phys. Rev. Lett.*, 107:266404, Dec 2011.
- [13] R. Arita, J. Kuneš, A. V. Kozhevnikov, A. G. Eguluz, and M. Imada. Ab initio Studies on the Interplay between Spin-Orbit Interaction and Coulomb Correlation in Sr_2IrO_4 and Ba_2IrO_4 . *Phys. Rev. Lett.*, 108:086403, Feb 2012.
- [14] Hongbin Zhang, Kristjan Haule, and David Vanderbilt. Effective $J=1/2$ Insulating State in Ruddlesden-Popper Iridates: An LDA+DMFT Study. *Phys. Rev. Lett.*, 111:246402, Dec 2013.
- [15] Danfeng Li, Kyuho Lee, Bai Yang Wang, Motoki Osada, Samuel Crossley, Hye Ryoung Lee, Yi Cui, Yasuyuki Hikita, and Harold Y. Hwang. Superconductivity in an infinite-layer nickelate. *Nature*, 572(7771):624–627, 2019.
- [16] Michel Crespin, Pierre Levitz, and Lucien Gataineau. Reduced forms of LaNiO_3 perovskite. Part 1.—Evidence for new phases: $\text{La}_2\text{Ni}_2\text{O}_5$ and LaNiO_2 . *J. Chem. Soc., Faraday Trans. 2*, 79:1181–1194, 1983.
- [17] Pierre Levitz, Michel Crespin, and Lucien Gataineau. Reduced forms of LaNiO_3 perovskite. Part 2.—X-ray structure of LaNiO_2 and extended X-ray absorption fine structure study: local environment of monovalent nickel. *J. Chem. Soc., Faraday Trans. 2*, 79:1195–1203, 1983.
- [18] V. I. Anisimov, D. Bukhvalov, and T. M. Rice. Electronic

- structure of possible nickelate analogs to the cuprates. *Phys. Rev. B*, 59:7901–7906, Mar 1999.
- [19] Motoki Osada, Bai Yang Wang, Berit H. Goodge, Kyuho Lee, Hyeok Yoon, Keita Sakuma, Danfeng Li, Masashi Miura, Lena F. Kourkoutis, and Harold Y. Hwang. A Superconducting Praseodymium Nickelate with Infinite Layer Structure. *Nano Letters*, 20(8):5735–5740, 08 2020.
- [20] Motoki Osada, Bai Yang Wang, Kyuho Lee, Danfeng Li, and Harold Y. Hwang. Phase diagram of infinite layer praseodymium nickelate $\text{Pr}_{1-x}\text{Sr}_x\text{NiO}_2$ thin films. *Phys. Rev. Materials*, 4:121801, Dec 2020.
- [21] Motoki Osada, Bai Yang Wang, Berit H. Goodge, Shannon P. Harvey, Kyuho Lee, Danfeng Li, Lena F. Kourkoutis, and Harold Y. Hwang. Nickelate Superconductivity without Rare-Earth Magnetism: $(\text{La},\text{Sr})\text{NiO}_2$. *Advanced Materials*, 33(45):2104083, 2021.
- [22] Zeng Shengwei, Li Changjian, Chow Lin Er, Cao Yu, Zhang Zhaoting, Tang Chi Sin, Yin Xinmao, Lim Zhi Shih, Hu Junxiong, Yang Ping, and Ariando Ariando. Superconductivity in infinite-layer nickelate $\text{La}_{1-x}\text{Ca}_x\text{NiO}_2$ thin films. *Science Advances*, 8(7):eabl9927, 2022.
- [23] Y. Maeno, H. Hashimoto, K. Yoshida, S. Nishizaki, T. Fujita, J. G. Bednorz, and F. Lichtenberg. Superconductivity in a layered perovskite without copper. *Nature*, 372(6506):532–534, 1994.
- [24] M. R. Norman. Entering the Nickel Age of Superconductivity. *Physics*, 13:85, 2020.
- [25] Warren E. Pickett. The dawn of the nickel age of superconductivity. *Nature Reviews Physics*, 3(1):7–8, 2021.
- [26] Junjie Zhang and Xutang Tao. Review on quasi-2D square planar nickelates. *CrystEngComm*, 23:3249–3264, 2021.
- [27] A. S. Botana, F. Bernardini, and A. Cano. Nickelate Superconductors: An Ongoing Dialog between Theory and Experiments. *Journal of Experimental and Theoretical Physics*, 132(4):618–627, 2021.
- [28] M. Azuma, Z. Hiroi, M. Takano, Y. Bando, and Y. Takeda. Superconductivity at 110 K in the infinite-layer compound $(\text{Sr}_{1-x}\text{Ca}_x)_{1-y}\text{CuO}_2$. *Nature*, 356(6372):775–776, 1992.
- [29] Koichi Momma and Fujio Izumi. VESTA3 for three-dimensional visualization of crystal, volumetric and morphology data. *J. Appl. Crystallogr.*, 44(6):1272–1276, Dec 2011.
- [30] Danfeng Li, Bai Yang Wang, Kyuho Lee, Shannon P. Harvey, Motoki Osada, Berit H. Goodge, Lena F. Kourkoutis, and Harold Y. Hwang. Superconducting Dome in $\text{Nd}_{1-x}\text{Sr}_x\text{NiO}_2$ Infinite Layer Films. *Phys. Rev. Lett.*, 125:027001, Jul 2020.
- [31] Shengwei Zeng, Chi Sin Tang, Xinmao Yin, Changjian Li, Mengsha Li, Zhen Huang, Junxiong Hu, Wei Liu, Ganesh Ji Omar, Hariom Jani, Zhi Shih Lim, Kun Han, Dongyang Wan, Ping Yang, Stephen John Pennycook, Andrew T. S. Wee, and Ariando Ariando. Phase Diagram and Superconducting Dome of Infinite-Layer $\text{Nd}_{1-x}\text{Sr}_x\text{NiO}_2$ Thin Films. *Phys. Rev. Lett.*, 125:147003, Oct 2020.
- [32] Kyuho Lee, Berit H. Goodge, Danfeng Li, Motoki Osada, Bai Yang Wang, Yi Cui, Lena F. Kourkoutis, and Harold Y. Hwang. Aspects of the synthesis of thin film superconducting infinite-layer nickelates. *APL Materials*, 8(4):041107, 2020.
- [33] Qiangqiang Gu, Yueying Li, Siyuan Wan, Huazhou Li, Wei Guo, Huan Yang, Qing Li, Xiyu Zhu, Xiaoqing Pan, Yuefeng Nie, and Hai-Hu Wen. Single particle tunneling spectrum of superconducting $\text{Nd}_{1-x}\text{Sr}_x\text{NiO}_2$ thin films. *Nat. Commun.*, 11(1):6027, 2020.
- [34] Qiang Gao, Yuchen Zhao, Xing-Jiang Zhou, and Zhihai Zhu. Preparation of Superconducting Thin Films of Infinite-Layer Nickelate $\text{Nd}_{0.8}\text{Sr}_{0.2}\text{NiO}_2$. *Chinese Physics Letters*, 38(7):077401, 2021.
- [35] Xiao-Rong Zhou, Ze-Xin Feng, Pei-Xin Qin, Han Yan, Xiao-Ning Wang, Pan Nie, Hao-Jiang Wu, Xin Zhang, Hong-Yu Chen, Zi-Ang Meng, Zeng-Wei Zhu, and Zhi-Qi Liu. Negligible oxygen vacancies, low critical current density, electric-field modulation, in-plane anisotropic and high-field transport of a superconducting $\text{Nd}_{0.8}\text{Sr}_{0.2}\text{NiO}_2/\text{SrTiO}_3$ heterostructure. *Rare Metals*, 2021.
- [36] Yueying Li, Wenjie Sun, Jiangfeng Yang, Xiangbin Cai, Wei Guo, Zhengbin Gu, Ye Zhu, and Yuefeng Nie. Impact of Cation Stoichiometry on the Crystalline Structure and Superconductivity in Nickelates. *Frontiers in Physics*, 9:443, 2021.
- [37] Xiao-Rong Zhou, Ze-Xin Feng, Pei-Xin Qin, Han Yan, Shuai Hu, Hui-Xin Guo, Xiao-Ning Wang, Hao-Jiang Wu, Xin Zhang, Hong-Yu Chen, Xue-Peng Qiu, and Zhi-Qi Liu. Absence of superconductivity in $\text{Nd}_{0.8}\text{Sr}_{0.2}\text{NiO}_x$ thin films without chemical reduction. *Rare Metals*, 39(4):368–374, 2020.
- [38] Liang Si, Wen Xiao, Josef Kaufmann, Jan M. Tomczak, Yi Lu, Zhicheng Zhong, and Karsten Held. Topotactic Hydrogen in Nickelate Superconductors and Akin Infinite-Layer Oxides ABO_2 . *Phys. Rev. Lett.*, 124:166402, Apr 2020.
- [39] Qing Li, Chengping He, Jin Si, Xiyu Zhu, Yue Zhang, and Hai-Hu Wen. Absence of superconductivity in bulk $\text{Nd}_{1-x}\text{Sr}_x\text{NiO}_2$. *Communications Materials*, 1(1):16, 2020.
- [40] Bi-Xia Wang, Hong Zheng, E. Krivyakina, O. Chmaissem, Pietro Papa Lopes, J. W. Lynn, Leighanne C. Gallington, Y. Ren, S. Rosenkranz, J. F. Mitchell, and D. Phelan. Synthesis and characterization of bulk $\text{Nd}_{1-x}\text{Sr}_x\text{NiO}_2$ and $\text{Nd}_{1-x}\text{Sr}_x\text{NiO}_3$. *Phys. Rev. Materials*, 4:084409, Aug 2020.
- [41] Chengping He, Xue Ming, Qing Li, Xiyu Zhu, Jin Si, and Hai-Hu Wen. Synthesis and physical properties of perovskite $\text{Sm}_{1-x}\text{Sr}_x\text{NiO}_3$ ($x = 0, 0.2$) and infinite-layer $\text{Sm}_{0.8}\text{Sr}_{0.2}\text{NiO}_2$ nickelates. *J. Phys.: Condens. Matter*, 33(26):265701, may 2021.
- [42] Pascal Puphal, Yu-Mi Wu, Katrin Fürsich, Hangoo Lee, Mohammad Pakdaman, Jan A. N. Bruin, Jürgen Nuss, Y. Eren Suyolcu, Peter A. van Aken, Bernhard Keimer, Masahiko Isobe, and Matthias Hepting. Topotactic transformation of single crystals: From perovskite to infinite-layer nickelates. *Sci. Adv.*, 7(49):eabl8091, 2021.
- [43] Oleksandr I. Malyi, Julien Varignon, and Alex Zunger. Bulk NdNiO_2 is thermodynamically unstable with respect to decomposition while hydrogenation reduces the instability and transforms it from metal to insulator. *Phys. Rev. B*, 105:014106, Jan 2022.
- [44] Yu-Te Hsu, Bai Yang Wang, Maarten Berben, Danfeng Li, Kyuho Lee, Caitlin Duffy, Thom Ottenbros, Woo Jin Kim, Motoki Osada, Steffen Wiedmann, Harold Y. Hwang, and Nigel E. Hussey. Insulator-to-metal crossover near the edge of the superconducting dome in $\text{Nd}_{1-x}\text{Sr}_x\text{NiO}_2$. *Phys. Rev. Research*, 3:L042015, Nov 2021.
- [45] M.A. Hayward and M.J. Rosseinsky. Synthesis of the infinite layer Ni(I) phase NdNiO_{2+x} by low temperature reduction of NdNiO_3 with sodium hydride. *Solid State Sci.*, 5(6):839 – 850, 2003. International Conference on Inorganic Materials 2002.
- [46] J. Zaanen, G. A. Sawatzky, and J. W. Allen. Band gaps and electronic structure of transition-metal compounds. *Phys. Rev. Lett.*, 55:418–421, Jul 1985.
- [47] M. Hepting, D. Li, C. J. Jia, H. Lu, E. Paris, Y. Tseng,

- X. Feng, M. Osada, E. Been, Y. Hikita, Y. D. Chuang, Z. Hussain, K. J. Zhou, A. Nag, M. Garcia-Fernandez, M. Rossi, H. Y. Huang, D. J. Huang, Z. X. Shen, T. Schmitt, H. Y. Hwang, B. Moritz, J. Zaanen, T. P. Devereaux, and W. S. Lee. Electronic structure of the parent compound of superconducting infinite-layer nickelates. *Nature Materials*, 19(4):381–385, 2020.
- [48] Ying Fu, Le Wang, Hu Cheng, Shenghai Pei, Xuefeng Zhou, Jian Chen, Shaoheng Wang, Ran Zhao, Wenrui Jiang, Cai Liu, Mingyuan Huang, XinWei Wang, Yusheng Zhao, Dapeng Yu, Fei Ye, Shanmin Wang, and Jia-Wei Mei. Core-level x-ray photoemission and Raman spectroscopy studies on electronic structures in Mott-Hubbard type nickelate oxide NdNiO₂, 2019, arXiv:1911.03177.
- [49] Berit H. Goodge, Danfeng Li, Kyuho Lee, Motoki Osada, Bai Yang Wang, George A. Sawatzky, Harold Y. Hwang, and Lena F. Kourkoutis. Doping evolution of the Mott-Hubbard landscape in infinite-layer nickelates. *Proceedings of the National Academy of Sciences*, 118(2):e2007683118, 2021.
- [50] Zhuoyu Chen, Motoki Osada, Danfeng Li, Emily M. Been, Su-Di Chen, Makoto Hashimoto, Donghui Lu, Sung-Kwan Mo, Kyuho Lee, Bai Yang Wang, Fanny Rodolakis, Jessica L. McChesney, Chunjing Jia, Brian Moritz, Thomas P. Devereaux, Harold Y. Hwang, and Zhi-Xun Shen. Electronic structure of superconducting nickelates probed by resonant photoemission spectroscopy, 2021, arXiv:2106.03963.
- [51] Hai Lin, Dariusz Jakub Gawryluk, Yannick Maximilian Klein, Shangxiong Huangfu, Ekaterina Pomjakushina, Fabian von Rohr, and Andreas Schilling. Universal spin-glass behaviour in bulk LaNiO₂, PrNiO₂ and NdNiO₂. *New Journal of Physics*, 2021.
- [52] Yi Cui, Cong Li, Qing Li, Xiyu Zhu, Ze Hu, Yi feng Yang, Jinshan Zhang, Rong Yu, Hai-Hu Wen, and Weiqiang Yu. NMR Evidence of Antiferromagnetic Spin Fluctuations in Nd_{0.85}Sr_{0.15}NiO₂. *Chinese Physics Letters*, 38(6):067401, 2021.
- [53] D. Zhao, Y. B. Zhou, Y. Fu, L. Wang, X. F. Zhou, H. Cheng, J. Li, D. W. Song, S. J. Li, B. L. Kang, L. X. Zheng, L. P. Nie, Z. M. Wu, M. Shan, F. H. Yu, J. J. Ying, S. M. Wang, J. W. Mei, T. Wu, and X. H. Chen. Intrinsic Spin Susceptibility and Pseudogaplike Behavior in Infinite-Layer LaNiO₂. *Phys. Rev. Lett.*, 126:197001, May 2021.
- [54] H. Lu, M. Rossi, A. Nag, M. Osada, D. F. Li, K. Lee, B. Y. Wang, M. Garcia-Fernandez, S. Agrestini, Z. X. Shen, E. M. Been, B. Moritz, T. P. Devereaux, J. Zaanen, H. Y. Hwang, Ke-Jin Zhou, and W. S. Lee. Magnetic excitations in infinite-layer nickelates. *Science*, 373(6551):213–216, 2021.
- [55] Priyo Adhikary, Subhadeep Bandyopadhyay, Tanmoy Das, Indra Dasgupta, and Tanusri Saha-Dasgupta. Orbital-selective superconductivity in a two-band model of infinite-layer nickelates. *Phys. Rev. B*, 102:100501, Sep 2020.
- [56] Zhan Wang, Guang-Ming Zhang, Yi-feng Yang, and Fu-Chun Zhang. Distinct pairing symmetries of superconductivity in infinite-layer nickelates. *Phys. Rev. B*, 102:220501, Dec 2020.
- [57] Naoya Kitamine, Masayuki Ochi, and Kazuhiko Kuroki. Designing nickelate superconductors with d^8 configuration exploiting mixed-anion strategy. *Phys. Rev. Research*, 2:042032, Nov 2020.
- [58] Xianxin Wu, Kun Jiang, Domenico Di Sante, Werner Hanke, A. P. Schnyder, Jiangping Hu, and Ronny Thomale. Surface s -wave superconductivity for oxide-terminated infinite-layer nickelates, 2020, arXiv:2008.06009.
- [59] Bai Yang Wang, Danfeng Li, Berit H. Goodge, Kyuho Lee, Motoki Osada, Shannon P. Harvey, Lena F. Kourkoutis, Malcolm R. Beasley, and Harold Y. Hwang. Isotropic Pauli-limited superconductivity in the infinite-layer nickelate Nd_{0.775}Sr_{0.225}NiO₂. *Nat. Phys.*, 17(4):473–477, 2021.
- [60] Ying Xiang, Qing Li, Yueying Li, Huan Yang, Yuefeng Nie, and Hai-Hu Wen. Physical Properties Revealed by Transport Measurements for Superconducting Nd_{0.8}Sr_{0.2}NiO₂ Thin Films. *Chinese Phys. Lett.*, 38(4):047401, may 2021.
- [61] M. Rossi, H. Lu, A. Nag, D. Li, M. Osada, K. Lee, B. Y. Wang, S. Agrestini, M. Garcia-Fernandez, J. J. Kas, Y.-D. Chuang, Z. X. Shen, H. Y. Hwang, B. Moritz, Ke-Jin Zhou, T. P. Devereaux, and W. S. Lee. Orbital and spin character of doped carriers in infinite-layer nickelates. *Phys. Rev. B*, 104:L220505, Dec 2021.
- [62] S. W. Zeng, X. M. Yin, C. J. Li, L. E. Chow, C. S. Tang, K. Han, Z. Huang, Y. Cao, D. Y. Wan, Z. T. Zhang, Z. S. Lim, C. Z. Diao, P. Yang, A. T. S. Wee, S. J. Pennycook, and A. Ariando. Observation of perfect diamagnetism and interfacial effect on the electronic structures in infinite layer Nd_{0.8}Sr_{0.2}NiO₂ superconductors. *Nature Communications*, 13(1):743, 2022.
- [63] Yusuke Nomura, Motoaki Hirayama, Terumasa Tadano, Yoshihide Yoshimoto, Kazuma Nakamura, and Ryotaro Arita. Formation of a two-dimensional single-component correlated electron system and band engineering in the nickelate superconductor NdNiO₂. *Phys. Rev. B*, 100:205138, Nov 2019.
- [64] Mitsuaki Kawamura. FermiSurfer: Fermi-surface viewer providing multiple representation schemes. *Comput. Phys. Commun.*, 239:197 – 203, 2019.
- [65] K.-W. Lee and W. E. Pickett. Infinite-layer LaNiO₂: Ni¹⁺ is not Cu²⁺. *Phys. Rev. B*, 70:165109, Oct 2004.
- [66] A. S. Botana and M. R. Norman. Similarities and Differences between LaNiO₂ and CaCuO₂ and Implications for Superconductivity. *Phys. Rev. X*, 10:011024, Feb 2020.
- [67] Hirofumi Sakakibara, Hidetomo Usui, Katsuhiko Suzuki, Takao Kotani, Hideo Aoki, and Kazuhiko Kuroki. Model Construction and a Possibility of Cuprate-like Pairing in a New d^9 Nickelate Superconductor (Nd,Sr)NiO₂. *Phys. Rev. Lett.*, 125:077003, Aug 2020.
- [68] Xianxin Wu, Domenico Di Sante, Tilman Schwemmer, Werner Hanke, Harold Y. Hwang, Srinivas Raghu, and Ronny Thomale. Robust $d_{x^2-y^2}$ -wave superconductivity of infinite-layer nickelates. *Phys. Rev. B*, 101:060504, Feb 2020.
- [69] Fabio Bernardini and Andres Cano. Stability and electronic properties of LaNiO₂/SrTiO₃ heterostructures. *Journal of Physics: Materials*, 2020.
- [70] Benjamin Geisler and Rossitza Pentcheva. Fundamental difference in the electronic reconstruction of infinite-layer versus perovskite neodymium nickelate films on SrTiO₃(001). *Phys. Rev. B*, 102:020502, Jul 2020.
- [71] Benjamin Geisler and Rossitza Pentcheva. Correlated interface electron gas in infinite-layer nickelate versus cuprate films on SrTiO₃(001). *Phys. Rev. Research*, 3:013261, Mar 2021.
- [72] Ri He, Peiheng Jiang, Yi Lu, Yidao Song, Mingxing Chen, Mingliang Jin, Lingling Shui, and Zhicheng Zhong. Polarity-induced electronic and atomic reconstruction at NdNiO₂/SrTiO₃ interfaces. *Phys. Rev. B*, 102:035118, Jul 2020.
- [73] Yang Zhang, Ling-Fang Lin, Wenjun Hu, Adriana Moreo, Shuai Dong, and Elbio Dagotto. Similarities and differences between nickelate and cuprate films grown on a SrTiO₃ substrate. *Phys. Rev. B*, 102:195117, Nov

- 2020.
- [74] T. Siegrist, S. M. Zahurak, D. W. Murphy, and R. S. Roth. The parent structure of the layered high-temperature superconductors. *Nature*, 334(6179):231–232, 1988.
- [75] K. Held. Electronic structure calculations using dynamical mean field theory. *Advances in Physics*, 56(6):829–926, 2007.
- [76] Yuhao Gu, Sichen Zhu, Xiaoxuan Wang, Jiangping Hu, and Hanghui Chen. A substantial hybridization between correlated Ni- d orbital and itinerant electrons in infinite-layer nickelates. *Communications Physics*, 3(1):84, 2020.
- [77] Motoaki Hirayama, Terumasa Tadano, Yusuke Nomura, and Ryotaro Arita. Materials design of dynamically stable d^9 layered nickelates. *Phys. Rev. B*, 101:075107, Feb 2020.
- [78] Emily Been, Wei-Sheng Lee, Harold Y. Hwang, Yi Cui, Jan Zaanen, Thomas Devereaux, Brian Moritz, and Chunjing Jia. Electronic Structure Trends Across the Rare-Earth Series in Superconducting Infinite-Layer Nickelates. *Phys. Rev. X*, 11:011050, Mar 2021.
- [79] Jesse Kapteghian and Antia S. Botana. Electronic structure and magnetism in infinite-layer nickelates $R\text{NiO}_2$ ($R = \text{La-Lu}$). *Phys. Rev. B*, 102:205130, Nov 2020.
- [80] Peiheng Jiang, Liang Si, Zhaoliang Liao, and Zhicheng Zhong. Electronic structure of rare-earth infinite-layer $R\text{NiO}_2$ ($R = \text{La, Nd}$). *Phys. Rev. B*, 100:201106, Nov 2019.
- [81] Mi-Young Choi, Kwan-Woo Lee, and Warren E. Pickett. Role of $4f$ states in infinite-layer NdNiO_2 . *Phys. Rev. B*, 101:020503, Jan 2020.
- [82] Ruiqi Zhang, Christopher Lane, Bahadur Singh, Johannes Nokelainen, Bernardo Barbiellini, Robert S. Markiewicz, Arun Bansil, and Jianwei Sun. Magnetic and f -electron effects in LaNiO_2 and NdNiO_2 nickelates with cuprate-like $3d_{x^2-y^2}$ band. *Communications Physics*, 4(1):118, 2021.
- [83] Subhadeep Bandyopadhyay, Priyo Adhikary, Tanmoy Das, Indra Dasgupta, and Tanusri Saha-Dasgupta. Superconductivity in infinite-layer nickelates: Role of f orbitals. *Phys. Rev. B*, 102:220502, Dec 2020.
- [84] Valerio Olevano, Fabio Bernardini, Xavier Blase, and Andrés Cano. Ab initio many-body GW correlations in the electronic structure of LaNiO_2 . *Phys. Rev. B*, 101:161102, Apr 2020.
- [85] Andrey L. Kutepov. Electronic structure of LaNiO_2 and CaCuO_2 from a self-consistent vertex-corrected GW approach. *Phys. Rev. B*, 104:085109, Aug 2021.
- [86] Antoine Georges, Gabriel Kotliar, Werner Krauth, and Marcelo J. Rozenberg. Dynamical mean-field theory of strongly correlated fermion systems and the limit of infinite dimensions. *Rev. Mod. Phys.*, 68:13–125, Jan 1996.
- [87] G. Kotliar, S. Y. Savrasov, K. Haule, V. S. Oudovenko, O. Parcollet, and C. A. Marianetti. Electronic structure calculations with dynamical mean-field theory. *Rev. Mod. Phys.*, 78:865–951, Aug 2006.
- [88] Siheon Ryee, Hongkee Yoon, Taek Jung Kim, Min Yong Jeong, and Myung Joon Han. Induced magnetic two-dimensionality by hole doping in the superconducting infinite-layer nickelate $\text{Nd}_{1-x}\text{Sr}_x\text{NiO}_2$. *Phys. Rev. B*, 101:064513, Feb 2020.
- [89] Philipp Werner and Shintaro Hoshino. Nickelate superconductors: Multiorbital nature and spin freezing. *Phys. Rev. B*, 101:041104, Jan 2020.
- [90] Motoharu Kitatani, Liang Si, Oleg Janson, Ryotaro Arita, Zhicheng Zhong, and Karsten Held. Nickelate superconductors—a renaissance of the one-band Hubbard model. *npj Quantum Materials*, 5(1):59, 2020.
- [91] Frank Lechermann. Late transition metal oxides with infinite-layer structure: Nickelates versus cuprates. *Phys. Rev. B*, 101:081110, Feb 2020.
- [92] Frank Lechermann. Multiorbital Processes Rule the $\text{Nd}_{1-x}\text{Sr}_x\text{NiO}_2$ Normal State. *Phys. Rev. X*, 10:041002, Oct 2020.
- [93] Frank Lechermann. Doping-dependent character and possible magnetic ordering of NdNiO_2 . *Phys. Rev. Materials*, 5:044803, Apr 2021.
- [94] Jonathan Karp, Antia S. Botana, Michael R. Norman, Hyowon Park, Manuel Zingl, and Andrew Millis. Many-Body Electronic Structure of NdNiO_2 and CaCuO_2 . *Phys. Rev. X*, 10:021061, Jun 2020.
- [95] Jonathan Karp, Alexander Hampel, Manuel Zingl, Antia S. Botana, Hyowon Park, Michael R. Norman, and Andrew J. Millis. Comparative many-body study of $\text{Pr}_4\text{Ni}_3\text{O}_8$ and NdNiO_2 . *Phys. Rev. B*, 102:245130, Dec 2020.
- [96] Jonathan Karp, Alexander Hampel, and Andrew J. Millis. Dependence of DFT + DMFT results on the construction of the correlated orbitals. *Phys. Rev. B*, 103:195101, May 2021.
- [97] I. Leonov, S. L. Skornyakov, and S. Y. Savrasov. Lifshitz transition and frustration of magnetic moments in infinite-layer NdNiO_2 upon hole doping. *Phys. Rev. B*, 101:241108, Jun 2020.
- [98] I. Leonov. Effect of lattice strain on the electronic structure and magnetic correlations in infinite-layer $(\text{Nd,Sr})\text{NiO}_2$. *Journal of Alloys and Compounds*, 883:160888, 2021.
- [99] Xiangang Wan, Vsevolod Ivanov, Giacomo Resta, Ivan Leonov, and Sergey Y. Savrasov. Exchange interactions and sensitivity of the Ni two-hole spin state to Hund’s coupling in doped NdNiO_2 . *Phys. Rev. B*, 103:075123, Feb 2021.
- [100] Y. Wang, C.-J. Kang, H. Miao, and G. Kotliar. Hund’s metal physics: From SrNiO_2 to LaNiO_2 . *Phys. Rev. B*, 102:161118, Oct 2020.
- [101] Chang-Jong Kang and Gabriel Kotliar. Optical Properties of the Infinite-Layer $\text{La}_{1-x}\text{Sr}_x\text{NiO}_2$ and Hidden Hund’s Physics. *Phys. Rev. Lett.*, 126:127401, Mar 2021.
- [102] Zhao Liu, Chenchao Xu, Chao Cao, W. Zhu, Z. F. Wang, and Jinlong Yang. Doping dependence of electronic structure of infinite-layer NdNiO_2 . *Phys. Rev. B*, 103:045103, Jan 2021.
- [103] Keisuke Higashi, Mathias Winder, Jan Kuneš, and Atsushi Hariki. Core-Level X-Ray Spectroscopy of Infinite-Layer Nickelate: LDA + DMFT Study. *Phys. Rev. X*, 11:041009, Oct 2021.
- [104] Francesco Petocchi, Viktor Christiansson, Fredrik Nilsson, Ferdi Aryasetiawan, and Philipp Werner. Normal State of $\text{Nd}_{1-x}\text{Sr}_x\text{NiO}_2$ from Self-Consistent GW + EDMFT. *Phys. Rev. X*, 10:041047, Dec 2020.
- [105] Byungkyun Kang, Corey Melnick, Patrick Semon, Siheon Ryee, Myung Joon Han, Gabriel Kotliar, and Sangkook Choi. Infinite-layer nickelates as Ni- e_g Hund’s metals, 2021, arXiv:2007.14610.
- [106] M. A. Hayward, M. A. Green, M. J. Rosseinsky, and J. Sloan. Sodium Hydride as a Powerful Reducing Agent for Topotactic Oxide Deintercalation: Synthesis and Characterization of the Nickel(I) Oxide LaNiO_2 . *J. Am. Chem. Soc.*, 121(38):8843–8854, 09 1999.
- [107] Hu Zhang, Lipeng Jin, Shanmin Wang, Bin Xi, Xingqiang Shi, Fei Ye, and Jia-Wei Mei. Effective Hamiltonian for nickelate oxides $\text{Nd}_{1-x}\text{Sr}_x\text{NiO}_2$. *Phys. Rev. Research*, 2:013214, Feb 2020.
- [108] Zhao Liu, Zhi Ren, Wei Zhu, Zhengfei Wang, and Jinlong Yang. Electronic and magnetic structure of infinite-layer NdNiO_2 : trace of antiferromagnetic metal. *npj Quantum Materials*, 5(1):31, 2020.

- [109] Zi-Jian Lang, Ruoshi Jiang, and Wei Ku. Strongly correlated doped hole carriers in the superconducting nickelates: Their location, local many-body state, and low-energy effective Hamiltonian. *Phys. Rev. B*, 103:L180502, May 2021.
- [110] Mi-Young Choi, Warren E. Pickett, and Kwan-Woo Lee. Fluctuation-frustrated flat band instabilities in NdNiO₂. *Phys. Rev. Research*, 2:033445, Sep 2020.
- [111] Patrick A. Lee, Naoto Nagaosa, and Xiao-Gang Wen. Doping a Mott insulator: Physics of high-temperature superconductivity. *Rev. Mod. Phys.*, 78:17–85, Jan 2006.
- [112] Mi Jiang, Mona Berciu, and George A. Sawatzky. Critical Nature of the Ni Spin State in Doped NdNiO₂. *Phys. Rev. Lett.*, 124:207004, May 2020.
- [113] Guang-Ming Zhang, Yi-Feng Yang, and Fu-Chun Zhang. Self-doped Mott insulator for parent compounds of nickelate superconductors. *Phys. Rev. B*, 101:020501, Jan 2020.
- [114] Yusuke Nomura, Takuya Nomoto, Motoaki Hirayama, and Ryotaro Arita. Magnetic exchange coupling in cuprate-analog d^9 nickelates. *Phys. Rev. Research*, 2:043144, Oct 2020.
- [115] Vamshi M. Katukuri, Nikolay A. Bogdanov, Oskar Weser, Jeroen van den Brink, and Ali Alavi. Electronic correlations and magnetic interactions in infinite-layer NdNiO₂. *Phys. Rev. B*, 102:241112, Dec 2020.
- [116] J. Bardeen, L. N. Cooper, and J. R. Schrieffer. Theory of Superconductivity. *Phys. Rev.*, 108:1175–1204, Dec 1957.
- [117] J.E. Hirsch and F. Marsiglio. Hole superconductivity in infinite-layer nickelates. *Physica C: Superconductivity and its Applications*, 566:1353534, 2019.
- [118] G. A. Sawatzky. Superconductivity seen in a non-magnetic nickel oxide. *Nature News and Views*, 572:592–593, 2019.
- [119] Ai Ikeda, Yoshiharu Krockenberger, Hiroshi Irie, Michio Naito, and Hideki Yamamoto. Direct observation of infinite NiO₂ planes in LaNiO₂ films. *Applied Physics Express*, 9(6):061101, may 2016.
- [120] Alexander Cyril Hewson. *The Kondo Problem to Heavy Fermions*. Cambridge Studies in Magnetism. Cambridge University Press, 1993.
- [121] F. C. Zhang and T. M. Rice. Effective Hamiltonian for the superconducting Cu oxides. *Phys. Rev. B*, 37:3759–3761, Mar 1988.
- [122] Ya-Hui Zhang and Ashvin Vishwanath. Type-II t - J model in superconducting nickelate Nd_{1-x}Sr_xNiO₂. *Phys. Rev. Research*, 2:023112, May 2020.
- [123] Lun-Hui Hu and Congjun Wu. Two-band model for magnetism and superconductivity in nickelates. *Phys. Rev. Research*, 1:032046, Dec 2019.
- [124] Jun Chang, Jize Zhao, and Yang Ding. Hund-Heisenberg model in superconducting infinite-layer nickelates. *The European Physical Journal B*, 93(12):220, 2020.
- [125] Yuki Matsumoto, Takafumi Yamamoto, Kousuke Nakano, Hiroshi Takatsu, Taito Murakami, Kenta Hongo, Ryo Maezono, Hiraku Ogino, Dongjoon Song, Craig M. Brown, Cédric Tassel, and Hiroshi Kageyama. High-Pressure Synthesis of A₂NiO₂Ag₂Se₂ (A=Sr, Ba) with a High-Spin Ni²⁺ in Square-Planar Coordination. *Angew. Chem. Int. Ed.*, 58(3):756–759, 2019.
- [126] Emilian M. Nica, Jyoti Krishna, Rong Yu, Qimiao Si, Antia S. Botana, and Onur Erten. Theoretical investigation of superconductivity in trilayer square-planar nickelates. *Phys. Rev. B*, 102:020504, Jul 2020.
- [127] For a review on multi-layer cuprates, see, e.g., Ref. [152].
- [128] Junjie Zhang, A. S. Botana, J. W. Freeland, D. Phelan, Hong Zheng, V. Pardo, M. R. Norman, and J. F. Mitchell. Large orbital polarization in a metallic square-planar nickelate. *Nat. Phys.*, 13(9):864–869, 2017.
- [129] J. Q. Lin, P. Villar Arribi, G. Fabbris, A. S. Botana, D. Meyers, H. Miao, Y. Shen, D. G. Mazzone, J. Feng, S. G. Chiuabian, A. Nag, A. C. Walters, M. García-Fernández, Ke-Jin Zhou, J. Pellicciari, I. Jarrige, J. W. Freeland, Junjie Zhang, J. F. Mitchell, V. Bisogni, X. Liu, M. R. Norman, and M. P. M. Dean. Strong Superexchange in a $d^{9-\delta}$ Nickelate Revealed by Resonant Inelastic X-Ray Scattering. *Phys. Rev. Lett.*, 126:087001, Feb 2021.
- [130] Z. Li, W. Guo, T. T. Zhang, J. H. Song, T. Y. Gao, Z. B. Gu, and Y. F. Nie. Epitaxial growth and electronic structure of Ruddlesden-Popper nickelates (La_{n+1}Ni_nO_{3n+1}, $n = 1-5$). *APL Materials*, 8(9):091112, 2020.
- [131] Wenjie Sun, Yueying Li, Xiangbin Cai, Jiangfeng Yang, Wei Guo, Zhengbin Gu, Ye Zhu, and Yuefeng Nie. Electronic and transport properties in Ruddlesden-Popper neodymium nickelates Nd_{n+1}Ni_nO_{3n+1} ($n = 1-5$). *Phys. Rev. B*, 104:184518, Nov 2021.
- [132] Y. Tokura and T. Arima. New classification method for layered copper oxide compounds and its application to design of new high Tc superconductors. *Jpn. J. Appl. Phys.*, 29:2388–2402, November 1990.
- [133] Victor Pardo and Antia S. Botana. Is there a proximate antiferromagnetic insulating phase in infinite-layer nickelates?, 2020, arXiv:2012.02711.
- [134] Bo-Xiao Zheng, Chia-Min Chung, Philippe Corboz, Georg Ehlers, Ming-Pu Qin, Reinhard M. Noack, Hao Shi, Steven R. White, Shiwei Zhang, and Garnet Kin-Lic Chan. Stripe order in the underdoped region of the two-dimensional Hubbard model. *Science*, 358(6367):1155–1160, 2017.
- [135] Andrew S. Darmawan, Yusuke Nomura, Youhei Yamaji, and Masatoshi Imada. Stripe and superconducting order competing in the Hubbard model on a square lattice studied by a combined variational Monte Carlo and tensor network method. *Phys. Rev. B*, 98:205132, Nov 2018.
- [136] Hong-Chen Jiang and Thomas P. Devereaux. Superconductivity in the doped Hubbard model and its interplay with next-nearest hopping t' . *Science*, 365(6460):1424–1428, 2019.
- [137] Kerstin Wissel, Ali Muhammad Malik, Sami Vasala, Sergi Plana-Ruiz, Ute Kolb, Peter R. Slater, Ivan da Silva, Lambert Alff, Jochen Rohrer, and Oliver Clemens. Topochemical Reduction of La₂NiO₃F₂: The First Ni-Based Ruddlesden-Popper $n=1$ T'-Type Structure and the Impact of Reduction on Magnetic Ordering. *Chemistry of Materials*, 32(7):3160–3179, 04 2020.
- [138] Y. Tsujimoto, C. I. Sathish, Y. Matsushita, K. Yamamura, and T. Uchikoshi. New members of layered oxychloride perovskites with square planar coordination: Sr₂MO₂Cl₂ ($M = \text{Mn, Ni}$) and Ba₂PdO₂Cl₂. *Chem. Commun.*, 50:5915–5918, 2014.
- [139] F Bernardini, V Olevano, X Blase, and A Cano. Infinite-layer fluoro-nickelates as d^9 model materials. *Journal of Physics: Materials*, 3(3):035003, jun 2020.
- [140] Zi-Jian Lang, Ruoshi Jiang, and Wei Ku. Proposal to improve Ni-based superconductors via enhanced charge transfer. *Phys. Rev. B*, 105:L100501, Mar 2022.
- [141] W. M. Li, J. F. Zhao, L. P. Cao, Z. Hu, Q. Z. Huang, X. C. Wang, Y. Liu, G. Q. Zhao, J. Zhang, Q. Q. Liu, R. Z. Yu, Y. W. Long, H. Wu, H. J. Lin, C. T. Chen, Z. Li, Z. Z. Gong, Z. Guguchia, J. S. Kim, G. R. Stewart, Y. J. Uemura, S. Uchida, and C. Q. Jin. Superconductivity in a unique type of copper oxide. *Proc. Natl. Acad. Sci. USA*, 116(25):12156–12160, 2019.
- [142] Hyo-Sun Jin, Warren E. Pickett, and Kwan-Woo Lee.

- Proposed ordering of textured spin singlets in a bulk infinite-layer nickelate. *Phys. Rev. Research*, 2:033197, Aug 2020.
- [143] A. S. Botana and M. R. Norman. Layered palladates and their relation to nickelates and cuprates. *Phys. Rev. Materials*, 2:104803, Oct 2018.
- [144] Jakub Gawraczyński, Dominik Kurzydłowski, Russell A. Ewings, Subrahmanyam Bandaru, Wojciech Gadamski, Zoran Mazej, Giampiero Ruani, Ilaria Bergenti, Tomasz Jaroń, Andrew Ozarowski, Stephen Hill, Piotr J. Leszczyński, Kamil Tokár, Mariana Derzsi, Paolo Barone, Krzysztof Wohlfeld, José Lorenzana, and Wojciech Grochala. Silver route to cuprate analogs. *Proc. Natl. Acad. Sci. USA*, 116(5):1495–1500, 2019.
- [145] B. Keimer, S. A. Kivelson, M. R. Norman, S. Uchida, and J. Zaanen. From quantum matter to high-temperature superconductivity in copper oxides. *Nature*, 518(7538):179–186, 2015.
- [146] Grace A. Pan, Dan Ferenc Segedin, Harrison LaBollita, Qi Song, Emilian M. Nica, Berit H. Goodge, Andrew T. Pierce, Spencer Doyle, Steve Novakov, Denisse Córdova Carrizales, Alpha T. N'Diaye, Pádraic Shafer, Hanjong Paik, John T. Heron, Jarad A. Mason, Amir Yacoby, Lena F. Kourkoutis, Onur Erten, Charles M. Brooks, Antia S. Botana, and Julia A. Mundy. Superconductivity in a quintuple-layer square-planar nickelate. *Nature Materials*, 2021.
- [147] Matteo Rossi, Motoki Osada, Jaewon Choi, Stefano Agrestini, Daniel Jost, Yonghun Lee, Haiyu Lu, Bai Yang Wang, Kyuho Lee, Abhishek Nag, Yi-De Chuang, Cheng-Tai Kuo, Sang-Jun Lee, Brian Moritz, Thomas P. Devereaux, Zhi-Xun Shen, Jun-Sik Lee, Ke-Jin Zhou, Harold Y. Hwang, and Wei-Sheng Lee. A Broken Translational Symmetry State in an Infinite-Layer Nickelate, 2021, 2112.02484.
- [148] G. Krieger, L. Martinelli, S. Zeng, L. E. Chow, K. Kummer, R. Arpaia, M. Moretti Sala, N. B. Brookes, A. Ariando, N. Viart, M. Salluzzo, G. Ghiringhelli, and D. Preziosi. Charge and spin order dichotomy in NdNiO₂ driven by SrTiO₃ capping layer, 2021, 2112.03341.
- [149] Charles C. Tam, Jaewon Choi, Xiang Ding, Stefano Agrestini, Abhishek Nag, Bing Huang, Huiqian Luo, Mirian García-Fernández, Liang Qiao, and Ke-Jin Zhou. Charge density waves in infinite-layer ndnio₂ nickelates, 2021, 2112.04440.
- [150] Junjie Zhang, Yu-Sheng Chen, D. Phelan, Hong Zheng, M. R. Norman, and J. F. Mitchell. Stacked charge stripes in the quasi-2D trilayer nickelate La₄Ni₃O₈. *Proceedings of the National Academy of Sciences*, 113(32):8945–8950, 2016.
- [151] Junjie Zhang, D. M. Pajerowski, A. S. Botana, Hong Zheng, L. Harriger, J. Rodriguez-Rivera, J. P. C. Ruff, N. J. Schreiber, B. Wang, Yu-Sheng Chen, W. C. Chen, M. R. Norman, S. Rosenkranz, J. F. Mitchell, and D. Phelan. Spin Stripe Order in a Square Planar Trilayer Nickelate. *Phys. Rev. Lett.*, 122:247201, Jun 2019.
- [152] Hidekazu Mukuda, Sunao Shimizu, Akira Iyo, and Yoshio Kitaoka. High- T_c Superconductivity and Antiferromagnetism in Multilayered Copper Oxides – A New Paradigm of Superconducting Mechanism–. *Journal of the Physical Society of Japan*, 81(1):011008, 2012.